Research Square

Preprints are preliminary reports that have not undergone peer review.
They should not be considered conclusive, used to inform clinical practice,
or referenced by the media as validated information.

Total saponins from Jiegeng decoction reverse NSCLC cisplatin resistance via PI3K/AKT/NF-κB Pathway

Lei Shen
Hunan University of Traditional Chinese Medicine
Guang Chen
Hunan University of Traditional Chinese Medicine
Menqin Zhu
Hunan University of Traditional Chinese Medicine
Jinyu Li
Hunan University of Traditional Chinese Medicine
Yanfeng Yuan
Hunan University of Traditional Chinese Medicine
Chang Yi
Hunan University of Traditional Chinese Medicine
Wenlong Liu
Hunan University of Traditional Chinese Medicine
Xili Zhang
xiaoli610@126.com

Hunan University of Traditional Chinese Medicine

Article

Keywords: Platycodon Decoction, Cisplatin resistance, Non-small cell lung cancer, PI3K/AKT/NF-κB pathway, Pharmacodynamic substances

Posted Date: September 21st, 2026

DOI: https://doi.org/10.21203/rs.3.rs-10681322/v1

License: This work is licensed under a Creative Commons Attribution 4.0 International License.
Read Full License

Additional Declarations: No competing interests reported.

Total saponins from Jiegeng decoction reverse NSCLC cisplatin resistance via PI3K/AKT/NF-κB Pathway

Lei Shen [1,2,3], Guang Chen[1,2,3], Mengqin Zhu[1,2,3], Jinyu Li[1,2,3], Yanfeng Yuan[1,2,3], Chang Yi[1,2,3], Wenlong Liu [1,2,3], and Xili Zhang [1,2,3,*]

[1] College of Pharmacy, Hunan University of Chinese Medicine, Changsha, 410208, China;
[2] Hunan Key Laboratory of Druggability and Preparation Modification of TCM, Changsha, 410208, China;
[3] Changsha Traditional Chinese Medicine Quality System Evaluation and Control and Precision Medication Technology Innovation Centre, Changsha, 410208, China
* Correspondence:dragon5240@126.com;xiaoli610@126.com

Abstract

Objective: Cisplatin resistance hinders NSCLC treatment. JGD shows potential to reverse chemoresistance, but its active fractions and mechanisms are unknown. We aimed to identify the optimal bioactive fraction and elucidate its mechanism. **Methods:** Total saponins, flavonoids, and polysaccharides were purified from JGD. Network pharmacology and molecular docking predicted core targets/pathways. Effects on cisplatin sensitivity were evaluated in A549/DDP cells using CCK-8, wound-healing, flow cytometry, and western blot. **Results:** Network pharmacology identified PI3K/AKT/NF-κB as the core pathway, with PIK3CA, AKT1, NFKB1 as key targets. All three fractions inhibited proliferation/migration and induced apoptosis. Total saponins combined with cisplatin reduced IC_{50} from 22.91±0.29 to 10.21±0.20 μM (reversal fold 2.24) and increased apoptosis from 21.45% to 50.26% (q=1.38). Mechanistically, all fractions downregulated PI3K, p-AKT, and NF-κB p65, with saponins most potent. **Conclusions:** Total saponins are the principal active fraction reversing cisplatin resistance via PI3K/AKT/NF-κB inhibition, supporting precise application of JGD and development of saponin-based sensitizers.

Keywords: Platycodon Decoction; Cisplatin resistance; Non-small cell lung cancer; PI3K/AKT/NF-κB pathway; Pharmacodynamic substances

1. Introduction

Lung cancer is a malignant tumor with the highest incidence and mortality rates worldwide. Non-small cell lung cancer (NSCLC) accounts for more than 85% of all lung cancers and is a major threat to human health (1). Although targeted therapy has become an important treatment for advanced NSCLC, its application is strictly dependent on mutations in driver genes, such as EGFR, ALK, and ROS1; it is ineffective for patients without these mutations and is expensive, limiting its clinical accessibility (2-4). Therefore, cisplatin (DDP)-based combination chemotherapy remains the first-line treatment for NSCLC. However, cisplatin resistance commonly develops during treatment, significantly reducing its efficacy and leading to recurrence and metastasis, presenting a critical clinical challenge that urgently needs to be addressed (5).

In recent years, traditional Chinese medicine (TCM) has demonstrated unique advantages in reversing chemoresistance in cancer. Numerous TCM formulas and natural products can restore tumor cell sensitivity to chemotherapy drugs through the synergistic action of multiple components, targets, and pathways, while offering high safety and minimal side effects (6). The Jiegeng Decoction, derived from Zhang Zhongjing's *Treatise on Cold Damage*, consists of a combination of Platycodon grandiflorus and Glycyrrhiza uralensis. It promotes lung function and soothes the throat, clearing heat, detoxifying, and eliminating phlegm and pus, making it a classic formula for treating pulmonary diseases (7, 8). Modern research has confirmed that Jiegeng Decoction can in-

hibit the proliferation and migration of lung cancer cells and promote apoptosis; when used in combination with cisplatin, it can significantly reverse the drug resistance of A549/DDP-resistant cells (9, 10); Its main active components include triterpene saponins, flavonoids, and polysaccharides, among which Platycodon saponin D, glycyrrhizic acid, and glycyrrhizin have all been reported to enhance sensitivity to chemotherapy (11, 12). Liquoric acid can inhibit the invasion of drug-resistant lung cancer cells by regulating the JAK2/STAT3 pathway, while glycyrrhizin B can synergize with cisplatin to promote tumor cell apoptosis, providing preliminary evidence for the use of Platycodon Decoction as a chemotherapeutic sensitizer (13, 14).

Previous studies have clearly demonstrated that abnormal activation of the PI3K/AKT/NF-κB signaling pathway is a key molecular mechanism underlying cisplatin resistance in lung cancer (15-18). Persistent activation of the PI3K/AKT pathway activates downstream NF-κB, which in turn upregulates drug efflux pumps such as P-gp and MRP1, as well as anti-apoptotic proteins such as Bcl-2 and XIAP, while suppressing the expression of the pro-apoptotic protein Bax, ultimately leading to the development of a drug-resistant phenotype (15, 19-21). Targeted inhibition of the PI3K/AKT/NF-κB pathway can effectively restore the sensitivity of drug-resistant cells to cisplatin and represents an ideal intervention target for reversing drug resistance (22, 23). Although the Jiegeng Decoction shows great potential for reversing lung cancer drug resistance, issues such as unclear active constituents, an undefined mechanism of action, and imprecise target pathways remain unresolved, significantly limiting its clinical translation and modern development. Existing studies have largely focused on the role of Jiegeng Decoction in chronic obstructive pulmonary disease (COPD), and systematic research on how its various bioactive components reverse cisplatin resistance in lung cancer remains relatively scarce.

Against the backdrop of innovation through the integration of traditional Chinese medicine (TCM) and modern medicine, the theory of "systemic target-oriented diagnosis and treatment" offers new insights for precision research on TCM formulations (24-26). Guided by a holistic perspective combined with modern biomedical technologies, this theory integrates "disease diagnosis—syndrome differentiation—target identification" to enhance therapeutic efficacy and safety through multi-component, multi-target systemic interventions (27, 28). Based on this theory, this study utilized D101 macroporous adsorption resin to optimize the separation and purification process for total flavonoids, total polysaccharides, and total saponins from Jiegeng Decoction and established quality control methods (29). Network pharmacology and molecular docking were employed to screen for core active components, key targets, and signaling pathways; further, using A549/DDP cisplatin-resistant cells as a model, we conducted CCK-8, cell scratch assays, flow cytometry, and western blot experiments to systematically evaluate the effects of different bioactive components of Jiegeng Decoction, both alone and in combination with cisplatin, on cell proliferation, migration, apoptosis, and the regulation of the PI3K/AKT/NF-κB pathway, elucidating the material basis and molecular mechanisms underlying their ability to reverse drug resistance. This study provides a scientific basis for the precise clinical application of the Jiegeng Decoction and the development of novel TCM chemotherapeutic sensitizers, while also offering a research model that can serve as a reference for the modernization of classical herbal formulas.

2. Materials and Methods

2.1. Experimental Herbal Materials

Platycodon is the dried root of Platycodon grandiflorum (Jacq.) A.DC. (Campanulaceae), and licorice is the dried root and rhizome of Glycyrrhiza uralensis Fisch. (family Fabaceae). Both were purchased from Jiuzhitang Co., Ltd. (Changsha, China) and were identified to comply with the relevant provisions of Part I of the 2025 Edition of the Chinese Pharmacopoeia (30). The herbal samples were stored in the laboratory.

2.2 Experimental Cells

The human lung cancer cisplatin-resistant cell line A549/DDP used in this experiment was purchased from Changsha Qicheng Biotechnology Co., Ltd., China, lot number: 20250702; the human lung cancer cell line A549 was purchased from Shanghai Jingxiang Qidian Biotechnology Co., Ltd., lot number: iCell-holl.

2.3 Experimental Reagents

The names, lot numbers, and manufacturers of the primary chemical reagents, antibodies, and cell culture consumables used in this study are listed in Table 1.

Reagent Name	**Lot Number**	**Manufacturer**
Platycodin D	20080723	Shanghai yuanye Bio-Technology Co., Ltd.
Glycyrrhizic acid	B201417	Shanghai yuanye Bio-Technology Co., Ltd.
Rutin	1000080-20181	Shanghai yuanye Bio-Technology Co., Ltd.
Anhydrous glucose	B21882	Shanghai yuanye Bio-Technology Co., Ltd.
Methanol (AR)	23045187	Tedia Company, Inc.
Acetonitrile (AR)	23085371	Tedia Company, Inc
Cisplatin (DDP)	HY-17394	MedChemExpress Biotechnology, Inc
Fetal bovine serum	24EO1000	Wuhan Pricella Biotechnology Co., Ltd.
F-12 medium	6125272	Wuhan Pricella Biotechnology Co., Ltd.
Penicillin-streptomycin	24EE0300	Wuhan Pricella Biotechnology Co., Ltd.
Trypsin	25AM0500	Wuhan Pricella Biotechnology Co., Ltd.
PBS buffer	24Fo1000	Wuhan Pricella Biotechnology Co., Ltd.
DMSO	814O035	Wuhan Pricella Biotechnology Co., Ltd.
BCA protein quantification kit	BCA202411	Nanjing Novazene Biotechnology Co., Ltd.
TWEEN 20	T8360	Beijing Solarbio Science & Technology Co.,Ltd.
RIPA lysis buffer	20241201	Yeasen Biotechnology (Shanghai) Co., Ltd.
SDS-PAGE Gel Preparation Kit	PG120	Wuhan Seville Biotechnology Co., Ltd.
Glycine	G8200	Beijing Solarbio Science & Technology Co.,Ltd.
PVDF membrane (0.22 μm)	ISEQ12345	Cytiva, a U.S. company
PMSF (100 mM)	P0102	Beijing Solarbio Science & Technology Co.,Ltd.
Protein marker	M2210	Thermo Fisher Scientific
Electrophoresis buffer	EB1002	Wuhan Boster Biological Technology co.ltd
TRIS	T8060	Beijing Kulai Bo Technology Co., Ltd.
Phosphoprotein inhibitor	P1260	APExBIO, a U.S. company
β-actin	10025459	Affinity Biosciences
PI3K antibody	AF6241	Affinity Biosciences
AKT antibody	AF6261	Affinity Biosciences
NF-κB antibody	ER0815	Hua'an Biotechnology Co., Ltd.
HRP-conjugated goat anti-rabbit	111-035-003	Jackson ImmunoResearch
HRP-conjugated goat anti-mouse	SA00001-1	Proteintech Group, Inc

2.4 Experimental Equipment

The names and manufacturers of the primary instruments and equipment used in this study are listed in Table 2.

Instrument Name	Manufacturer
TU-1900 Dual-Beam UV-Vis Spectrophotometer	Beijing Puxi General Instrument Co., Ltd.
RE52-98 Rotating Evaporator	Shanghai Yarong Biochemical Instrument Factory
Constant-Temperature Water Bath	Jiangsu Jintan Ronghua Instrument Manufacturing Co., Ltd.
Freeze Dryer	Ningbo Xinzhi Biotechnology Co., Ltd.
KQ2200 Ultrasonic Cleaner	Shanghai Shunyu Hengping Scientific Instruments Co., Ltd.
Waters High-Performance Liquid Chromatograph	Waters Corporation
CO_2 Incubator	Thermo Fisher Scientific
Biological Safety Cabinet	Thermo Fisher Scientific
Centrifuge	Hunan Xiangli Instruments Co., Ltd.
MB580 Microplate Reader	Shenzhen Huisong Company
Inverted Fluorescence Microscope	Menji Biotechnology Co., Ltd.

2.5 Preparation and Quality Control of the Active Components in Jiegeng Decoction

2.5.1 Preparation of the Jiegeng Decoction Extract

Precise amounts of Platycodon grandiflorus and Glycyrrhiza uralensis crude slices according to the original formula proportions in *Treatise on Cold Damage Diseases* (Platycodon grandiflorus: Glycyrrhiza uralensis = 1:2 by mass) (31). Mix the ingredients, add 10 times the volume (mL/g) of distilled water, soak for 1 h, and then heat to boiling and extract for 1 h before filtering. Eight times the volume of distilled water was added to the residue, boiled for 1 h, and then filtered. The two filtrates were combined and concentrated via rotary evaporation. After stirring, four times the volume of anhydrous ethanol was added, stirred for 1 h, and allowed to stand overnight. The precipitate was the total polysaccharide fraction, which was then transferred to a mortar and dried at 45°C. Evaporate and concentrate the supernatant, extract with n-butanol, concentrate the aqueous layer, freeze dry, and set aside for later use (32).

2.5.2 Pretreatment of D101 Macroporous Adsorption Resin

The D101 macroporous adsorption resin was soaked in anhydrous ethanol for 24 h to allow it to swell thoroughly and then rinsed with distilled water until the rinse solution was free of any ethanol odor. The resin was soaked in a 5% HCl solution for 3–4 h and then washed with water until the solution was neutral. Next, the resin was soaked in a 5% NaOH solution (2–3 times the column volume) for 3–5 h and then washed with water until the solution was neutral to ensure that impurities were removed from the resin (33, 34).

2.5.3 Separation and Purification of Total Flavonoids and Total Polysaccharides

Total flavonoids from Platycodon Decoction were purified using D101 macroporous adsorption resin under the following conditions: static adsorption for 8 h, static desorption for 6 h, loading solution pH 5.0, and elution with 70% ethanol. The 70% ethanol eluate was collected, concentrated under reduced pressure, and freeze-dried to obtain the total flavonoid fraction of the Platycodon Decoction (32).

The concentrated decoction of Platycodon grandiflorus was loaded onto a D101 macroporous adsorption resin column under the following conditions: static adsorption for 8 h, static desorption for 6 h, sample pH 7.0, and elution with 50% ethanol. The 50% ethanol

eluate was collected, concentrated under reduced pressure, and freeze-dried to obtain the total polysaccharide fraction from the decoction of Platycodon grandiflorus. Additionally, the deionized water eluate collected during the purification of total flavonoids and polysaccharides was combined and concentrated under reduced pressure, and anhydrous ethanol was added to a final concentration of 80% (v/v). The mixture was allowed to stand overnight at 4°C to precipitate polysaccharides, which were collected by centrifugation, washed, and freeze-dried to obtain the total polysaccharide fraction (32).

2.5.4 Preparation of Total Saponins

Total saponins from the Jiegeng Decoction were prepared according to the method described in the literature (35), which was passed at a specific flow rate through a D101 macroporous adsorption resin column. After complete adsorption, the eluate was collected, concentrated to a specific volume using a rotary evaporator, and then freeze-dried to obtain the freeze-dried powder of total saponins from the Jiegeng Decoction.

2.5.5 Determination of Total Flavonoid Content

Total flavonoid content was determined using the aluminum nitrate–sodium nitrite colorimetric method (32). The rutin reference standard (5 mg) was precisely weighed, dissolved in 70% ethanol, and diluted to volume in a 10 mL volumetric flask to prepare the reference solution (0.5 mg/mL). An appropriate amount of freeze-dried Jiegeng Decoction powder was dissolved in 70% ethanol and diluted to volume to prepare the test solution.

The rutin standard solutions (0.0, 0.1, 0.2, 0.3, 0.4, 0.5, and 0.6 mL) were placed into 10-mL volumetric flasks and diluted to volume with anhydrous ethanol. Take 1 mL of each of the above solutions; add 0.5 mL of 5% $NaNO_2$ solution to each in sequence, mix well, and let stand for 6 min; add 0.5 mL of 10% $Al(NO_3)_3$ solution, mix well, and let stand for 6 min; add 4 mL of 4% NaOH solution, mix well, then make up to volume with anhydrous ethanol, and let stand for 15 min. Absorbance was measured at 508 nm and a standard curve was plotted with rutin concentration (mg/mL) on the x-axis and absorbance on the y-axis. The test samples were processed using the same method, after which the values were substituted into the standard curve to calculate the total flavonoid content, which was expressed as rutin equivalents (mg rutin/g extract).

2.5.6 Determination of Total Polysaccharide Content

Total polysaccharide content was determined using the anthrone-sulfuric acid method (32). Five milligrams of anhydrous glucose reference standard was weighed with precision, dissolved in purified water, and the volume was made up to 10 mL in a brown volumetric flask to obtain an anhydrous glucose reference solution (0.5 mg/mL). Accurately weigh 0.1 g) were accurately weighed from Jiegeng Decoction, placed in a 40-mL volumetric flask, dissolved in 70% ethanol, and made up to the mark. Shake well to obtain the test solution.

Accurately measure 0.0, 0.1, 0.2, 0.3, 0.4, 0.5, and 0.6 mL of the anhydrous glucose reference solution into 10-mL volumetric flasks, dilute with water to 2.0 mL, add 6 mL of 0.1% anthrone sulfate solution, mix thoroughly, boil in a boiling water bath for 2 min, cool to room temperature in an ice bath, and measure the absorbance at 610 nm. A standard curve was plotted with glucose concentration (mg/mL) on the x-axis and absorbance on the y-axis. The test

sample was processed using the same method. After measuring the absorbance, the value was substituted into the standard curve to calculate the total polysaccharide content. The results were expressed as glucose equivalents (mg glucose/g extract).

2.5.7 Determination of Total Saponins (Platycodin D and Glycyrrhizic Acid)

The platycodin D content in the total saponin fraction was determined using the HPLC-PDA method (35). The chromatographic conditions were as follows: C18 column (250 mm × 4.6 mm, 5 μm, Phenomenex Luna); mobile phase A was 0.1% aqueous phosphoric acid, and mobile phase B was pure acetonitrile. The gradient elution program was as follows: 0–5 min, 95% → 85% A; 5–15 min, 85% → 75% A; 15–25 min, 75% → 65% A; 25–35 min, 65% → 60% A; 35–55 min, 60% → 50% A; detection wavelength, 254 nm; column temperature, 25°C; injection volume, 10 μL; flow rate, 1 mL/min. Accurately weigh 3.01 mg of Platycodon glycoside D reference standard was accurately weighed, and methanol (chromatographic grade) to a 10 mL volumetric flask and diluted to volume to obtain a reference solution (0.301 mg/mL). First, freeze-dried powder (0.1 g) of total saponins from Platycodon grandiflorus decoction was placed in a 10 mL brown volumetric flask, dissolved in chromatographic-grade methanol, sonicated for 20 min, cooled, and made up to the mark. The supernatant through a 0.22 μm microporous filter membrane to obtain the test solution. The reference and test solutions were injected separately under the aforementioned chromatographic conditions for analysis and the peak areas were recorded. A standard curve was plotted with the peak area on the y-axis and the reference concentration on the x-axis. The content of Platycodin D in the total saponins of Jiegeng Decoction was based on the standard curve.

The glycyrrhizic acid content in the total saponins was determined using the HPLC-ELSD method (35). The chromatographic conditions were as follows: C18 column (250 mm × 4.6 mm, 5 μm); mobile phase of acetonitrile–0.1% formic acid in water (27:73, v/v), with isocratic elution for 30 min; ELSD detector nitrogen flow rate: 1.20 L/min; drift tube temperature, 60°C; injection volume, 10 μL. Accurately weigh 3.05 mg of glycyrrhizic acid reference standard, add methanol (chromatographic grade) was added to a 10 mL volumetric flask and diluted to volume to obtain a reference solution (0.305 mg/mL). Prepare the test solution as described in section “2.5.7.” The reference and test solutions were injected separately for analysis, and the peak areas were recorded. A standard curve was plotted with the peak area on the y-axis and the reference concentration on the x-axis. Glycyrrhizic acid content in the total saponins of Jiegeng Decoction based on the standard curve.

2.5.8 Method Validation

The UV and HPLC methods for determining the content described above were validated in accordance with the relevant requirements of the General Chapter (9101) of the 2025 Edition of the Chinese Pharmacopoeia (30), including linearity, precision (intra- and inter-day), repeatability, stability, and spiked recovery tests. All determinations were performed in triplicate, and the results are expressed as mean ± standard deviation (mean ± SD).

2.9 Network Pharmacology and Molecular Docking

2.9.1 Screening of Active Components and Target Prediction for Jiegeng Decoction

The TCMSP database (https://old.tcmsp-e.com/tcmsp.php) was used to screen for bioactive compounds in Platycodon Decoction derived from Platycodon grandiflorus and Glycyrrhiza uralensis, using oral bioavailability (OB) ≥ 30% and drug-like properties (DL) ≥ 0.18 as screening criteria (36, 37). The 2D structures of the screened bioactive compounds were imported into the Swiss Target Prediction database (http://www.swisstargetprediction.ch/), with the species set to "Homo sapiens," to identify corresponding targets. After merging the targets from Platycodon grandiflorus and Glycyrrhiza uralensis and removing duplicates, potential targets for the bioactive compounds in Jiegeng Decoction were identified (38, 39).

2.9.2 Screening of Targets Associated with Drug-Resistant Lung Cancer

Using the keyword "Drug-resistant lung cancer" in the Genecards database (https://www.genecards.org/), we identified target genes associated with Drug-resistant lung cancer (38). The active ingredient targets of Jiegeng Decoction and drug-resistant lung cancer targets were analyzed using the Venny 2.1.0 platform (http://www.liuxiaoyuyuan.cn/) to identify the intersection, thereby obtaining common targets, and a Venn diagram was plotted.

2.9.3 Construction of the "Active Ingredient–Disease Target" Network

The intersection of active ingredients in Jiegeng Decoction and drug-resistant lung cancer targets was imported into Cytoscape 3.10.1 software to construct a "Traditional Chinese Medicine Active Ingredient–Disease Target" network diagram for visualization. The top ten components ranked by degree were selected as the core active ingredients of Jiegeng Decoction for treating drug-resistant lung cancer (38).

2.9.4 Construction of the Protein-Protein Interaction (PPI) Network

The intersection of the active ingredients and drug-resistant lung cancer targets was imported into the STRING database (https://string-db.org/). The species was set to "Homo sapiens," the interaction score was set to >0.9, and the data source was selected as experimentally validated data. After excluding isolated nodes, the results were exported . tsv files (38). The file was imported into Cytoscape 3.10.1 for visualization. Targets were sorted by degree centrality (DC), and the top 10 targets by degree value were selected as the core targets for the treatment of drug-resistant lung cancer with Jiegeng Decoction.

2.9.5 GO Functional Enrichment and KEGG Pathway Enrichment Analysis

The intersection of targets was imported into the Metascape platform (https://metascape.org/) for GO functional enrichment analysis and KEGG pathway enrichment analysis(40-42), with the threshold set at $P < 0.05$ (37). The top 10 entries in the Biological Process (BP), Cellular Component (CC), and Molecular Function (MF) categories from the GO analysis as well as the top 20 entries from the KEGG analysis were selected. Bar charts and bubble charts were generated using the microbioinformatics platform (http://www.bioinformatics.com.cn/) for visualization.

2.9.6 Molecular Docking Validation

The 2D structures of the core active components (platycodin D, glycyrrhizin, isoglycyrrhizin, and glycyrrhetic acid) were obtained from PubChem (https://pubchem.ncbi.nlm.nih.gov/) and saved in SDF format. Energy minimization was performed using ChemDraw 20.0. mol2 format and then imported into AutoDock Tools 1.5.7 for preprocessing prior to docking (38).

The top ten receptor proteins ranked by their network pharmacology "moderation" scores were selected. The Entry numbers for each protein were obtained from the UniProt database (https://www.uniprot.org/) and the corresponding PDB files were downloaded from the RCSB database (https://www.rcsb.org/). Water molecules and non-target residues were removed using PyMOL, and the models were imported into AutoDock Tools 1.5.7 for hydrogenation, charge calculation, and other pre-processing steps (39).

In AutoDock Tools 1.5.7, a grid box was set to enclose the receptor proteins, and the file was saved . gpf format. Molecular docking was performed using AutoDock Vina to calculate the binding energy. A binding energy of < -5 kcal/mol indicates that the ligand has a good binding affinity with the receptor (38, 39). The docking results were visualized using PyMOL software to analyze the interaction patterns between the active ingredient and the target protein (e.g., hydrogen bonds and hydrophobic interactions).

2.10 Cell Experiments

2.10.1 Cell Lines and Culture Conditions

A549 cells were cultured in high-glucose DMEM containing 10% fetal bovine serum (FBS) and 1% penicillin-streptomycin solution. A549/DDP cells were cultured in Ham's F-12K medium containing 10% fetal bovine serum, 1% penicillin-streptomycin solution, and 1 μg/mL cisplatin (DDP) to maintain their drug-resistant phenotype. Both the cell lines were incubated at 37°C in a humidified incubator containing 5% CO_2. All cell-related operations were performed under aseptic conditions and cells in the logarithmic growth phase were selected for all experiments.

2.10.2 Preparation of the Various Groups of Platycodon Decoction

Freeze-dried powders of total polysaccharides (PPG), total flavonoids (FPG), and total saponins (SPG) from Jiegeng Decoction were weighed separately, dissolved in DMSO, and prepared as stock solutions at a concentration of 20 mg/mL. These solutions were sterilized by filtration through a 0.22 μm sterile filter membrane, aliquoted, and stored at −20°C for later use. Immediately before use, the solutions were diluted to the desired concentrations using complete culture medium. In all DMSO-treated groups, the final DMSO concentration did not exceed 0.1% to ensure no toxic effects on the cells.

2.10.3 Experimental Groups

To investigate the effects of total saponins, total flavonoids, total polysaccharides from Jiegeng Decoction, and cisplatin on A549/DDP cells, the experiment was divided into the following nine groups: ① Control group (blank control), ② DDP group (20 μM cisplatin), ③ FPG group (0.1 mg/mL total flavonoids), ④ SPG group (0.1 mg/mL total saponins), ⑤ PPG group (0.1 mg/mL total polysaccharides), ⑥ DDP+FPG group (20 μM cisplatin + 0.1 mg/mL

total flavonoids), ⑦ DDP+SPG group (20 μM cisplatin + 0.1 mg/mL total saponins), ⑧ DDP+PPG group (20 μM cisplatin + 0.1 mg/mL total polysaccharides), ⑨ DDP+PSF group (20 μM cisplatin + a composite fraction of total polysaccharides, total flavonoids, and total saponins).

2.10.4 Detection of Cell Proliferation Using the CCK-8 Assay

A549 and A549/DDP cells in logarithmic growth phase were harvested, digested, and counted. The cell density was adjusted to 5×10^4 cells/mL using complete medium and 100 μL was seeded into each well of a 96-well plate (approximately 5,000 cells per well). The plates were incubated for 24 h until cells adhered. Discard the original culture medium and add different concentrations of total polysaccharides, total flavonoids, and total saponins from Platycodon grandiflorus decoction (0.1, 0.2, 0.3, 0.4, 0.5, 0.6 mg/mL) to treat the cells. Three replicate wells were set up per group and cultured for 24 h. Add 10 μL of CCK-8 solution to each well and incubated in the incubator for 4 h. Absorbance (OD value) of each well was measured at 450 nm using a microplate reader, and the cell survival rate was calculated using the following formula (32):

Cell survival rate (%) = (OD value of the treated group − OD value of the blank group) / (OD value of the control group − OD value of the blank group) × 100

To evaluate the sensitizing effects of the various components of Jiegeng Decoction on cisplatin, 0.1 mg/mL of total polysaccharides, total flavonoids, and total saponins from Jiegeng Decoction were each combined with different concentrations of cisplatin (4, 8, 12, 16, 20, 24 μM). After 24 h of culture, 10 μL of CCK-8 solution was added to each well, followed by incubation for 4 h. Absorbance was measured at 450 nm using a microplate reader, and the cell survival rate and half-maximal inhibitory concentration (IC_{50}) of cisplatin were calculated. The experiment was independently repeated thrice.

2.10.5 Cell Scratch Assay

A549/DDP cells in the logarithmic growth phase were isolated, digested with trypsin, resuspended in complete medium, and counted to adjust the cell density to 2×10^5 cells/mL. Using a marker pen, three parallel lines were evenly spaced (0.5–1 cm apart) across the bottom of each well in a six-well plate. Two milliliters of cell suspension were seeded into each well and incubated in an incubator for 24 h until the cells adhered and completely covered the well. Using a 200 μL sterile pipette tip, a scratch was made perpendicular to the parallel lines at the bottom of the well, applying even pressure and completing the scratch in a single, smooth motion. the six-well plate 2 to three times with PBS to remove scraped floating cells. Take a photograph of the scraped area in each well under an inverted microscope and record the scratch width at 0 h. Subsequently, replace the medium with drug-containing serum-free medium according to the grouping described in Section “2.7.3” (to exclude the interference of cell proliferation on migration results), and continue culturing for 24 h and 48 h. Take photographs of the same scratch area again at the 24-h and 48-h time points, respectively. The images were analyzed using the ImageJ software to measure the scratch width and calculate the cell migration rate using the following formula: Repeat the experiment independently three times (32):

Cell migration rate (%) = (scratch width at 0 h − scratch width at 24 h (or 48 h)) / scratch width

at 0 h × 100.

2.10.6 Detection of Cell Apoptosis by Flow Cytometry

Take A549/DDP cells in good growth condition, count them after digestion according to the cell passaging procedure, and seed them into a 6-well plate at 2 mL of culture medium per well (cell density approximately 2×10^5 cells/well). The plate was gently shaken to distribute the cells evenly and was incubated at 37°C in a 5% CO_2 incubator for 24 h. Once the cells had adhered to the surface and reached an appropriate density, the culture medium was replaced with drug-containing medium according to the grouping described in Section 2.7.3, and cultured for 48 h. Suspended cells were collected from the supernatant, and adherent cells were digested with EDTA-free trypsin. Both cell suspensions were combined in a centrifuge tube and centrifuged at 1000 rpm for 5 min, and the supernatant was discarded. The cells were washed twice with pre-chilled phosphate-buffered saline (PBS). The cells were resuspended in 200 μL of 1× Binding Buffer, and 10 μL of Annexin V-FITC was added, mixed gently, and incubated at room temperature in the dark for 15 min. Next, 5 μL of PI staining solution was added and incubated at room temperature in the dark for another 15 min. The apoptosis rate was determined by flow cytometry within 1 h after the end of the incubation. Cells positive for Annexin V-FITC alone were early apoptotic cells; cells positive for PI alone were late apoptotic cells or necrotic cells; double-positive cells were late apoptotic cells; and cells negative for both Annexin V-FITC and PI were viable cells. Total apoptosis rate = early apoptosis rate + late apoptosis rate. The experiment was independently repeated thrice.

2.10.7 Western Blot Analysis of Protein Expression

Harvest A549/DDP cells in the logarithmic growth phase, digest them with trypsin, resuspend and count the cells, adjust the cell density to 2×10^5 cells/mL, and seed them into 10-cm culture dishes (approximately 2×10^6 cells per dish). The cells were cultured overnight until they adhered to the dish. Administer drugs according to the groupings specified in Section 2.4.6, and culture was continued for 24 h. Culture medium was discarded, and the cells were washed twice with pre-chilled PBS. Two hundred microliters of RIPA lysis buffer (containing 1% PMSF and a phosphoproteinase inhibitor) was added to each dish. Swirl the dish to ensure that the lysis buffer comes into contact with the cells. A cell scraper was used to push the lysis buffer to one side, collect it into a 1.5 mL Eppendorf tube, and place it on ice for 15 min to allow lysis. Centrifuge in a pre-chilled centrifuge at 4°C and 12,000 rpm for 15 min. The supernatant is the total protein sample. The protein concentration was determined using a BCA protein quantification kit. The protein sample was mixed with 5× protein loading buffer in a 4:1 (v/v) ratio, heated in a metal bath at 100°C for 10 min to denature the protein, and after cooling, used for western blot loading or aliquoted and store at -20°C.

The glass plates were washed with deionized water, allowed to air dry, and secured vertically in a gel rack. A separation gel of the appropriate concentration was prepared based on the molecular weight of the target protein, using a 10% separation gel for PI3K (85 kDa), a 12% separation gel for AKT (56 kDa), p-AKT (56 kDa), and NF-κB p65 (65 kDa), and a 10% or 12% separation gel for β-actin (42 kDa). 30% gel-casting solution (29:1), 1.5 M Tris-HCl (pH 8.8), 10% SDS, 10% ammonium persulfate (APS), and TEMED were mixed in the specified proportions, and the mixture was then poured between the glass plates. Anhydrous ethanol was

added to cap the gel and allowed to stand at room temperature for 30 min until the separating gel completely solidified. The anhydrous ethanol was discarded, rinsed with deionized water, and blotted. A 5% concentrating gel (30% gel-casting solution, 1 M Tris-HCl pH 6.8, 10% SDS, 10% APS, and TEMED) was prepared, poured over the separation gel, inserted into a clean, air-dried comb, and allowed to stand at room temperature for 20 min until the concentrated gel had completely solidified.

Secure the gel plate in the electrophoresis chamber and add 1× electrophoresis buffer (10× electrophoresis buffer diluted 10-fold with deionized water). The comb was carefully removed to ensure that the loading well remained intact. Load 25 μg of protein sample per group and add an equal volume of protein loading buffer to the loading wells on both sides to prevent edge effects. A pre-stained protein marker (10–180 kDa) was used as a molecular weight reference. Turn on the power. The voltage for the gel concentration phase was set to 75 V, and the gel was run for approximately 30 min until the bromophenol blue front entered the separation gel. The voltage for the separation phase was set to 100 V and the gel was run for approximately 90 min, stopping when the bromophenol blue front approached the bottom of the glass plate.

A wet transfer method was used in this study. The gel was trimmed to the size of the protein marker and placed in a transfer sandwich clamp. The PVDF membrane (0.22 μm or 0.45 μm) was activated with methanol for 10 s and then equilibrated with transfer buffer. The sandwich clamp was assembled in the following order: "sponge–filter paper–gel–PVDF membrane–filter paper–sponge," and gently rolled to remove air bubbles. The sandwich clamp was placed in the transfer chamber with the red side facing the red side and the black side facing the black side, filling the chamber with pre-chilled transfer buffer, and closing the lid. The transfer chamber was placed in a mixture of ice and water to maintain low temperature, and the transfer was performed at a constant current of 300 mA for 180 min.

After transfer, the PVDF membrane was removed and washed once with 1×TBST (10×TBST diluted 1:9 with deionized water). The PVDF membrane was placed in 1×TBST blocking solution containing 5% skim milk powder and blocked at room temperature in a shaking incubator for 1 h. After blocking, the membrane was washed three times with 1×TBST for 5 min each. The membrane was incubated with the appropriate primary antibodies (PI3K, AKT, p-AKT, NF-κB p65, or β-actin antibodies, all diluted 1:1000) overnight at 4°C in a shaking incubator. The next day, the primary antibody was removed and the membrane was washed three times with 1×TBST for 5 min each. Incubate the membrane with HRP-conjugated goat anti-rabbit or goat anti-mouse secondary antibody (dilution ratio 1:5000) at room temperature for 1 hour. After incubation, the membranes were washed six times with 1×TBST for 5 min each.

Finally, protein signals were detected using an enhanced chemiluminescence (ECL) kit, and exposed and developed using a chemiluminescence imaging system. All protein bands were normalized to β-actin as an internal control to ensure consistent loading across the samples. Band grayscale values were analyzed using the ImageJ software to calculate the relative expression levels of each protein and the p-AKT/AKT ratio. The experiment was independently repeated thrice.

2.11 Statistical Analysis

The experimental data were analyzed using GraphPad Prism 9.5 software. Quantitative data were expressed as mean ± standard deviation (mean ± SD). Comparisons among multiple groups were performed using one-way analysis of variance (ANOVA), while comparisons between two groups were performed using an independent sample t-test. Statistical significance was set at $P < 0.05$, while P-values <0.01 and <0.001 were considered highly statistically significant.

3 Results

3.1 Quality Control of the Active Constituents in Jiegeng Decoction

3.1.1 Results of Methodological Validation for Content Determination

The results of the methodological validation for the determination of the three categories of active constituents in Jiegeng Decoction are summarized in Table 3. The RSD values for precision, repeatability, stability, and spiked recovery of all the methods were less than 3%, meeting the relevant requirements of the General Rules (9101) of the 2025 Edition of the Chinese Pharmacopoeia (30). This indicates that the established methods are reliable and accurate and can be used for the quality control of the active constituents in Jiegeng Decoction.

Table 3 Summary of methodological validation results for the determination of the content of three components in Jiegeng Decoction.

Component	Test Parameters	Linear Equations	R^2	Precision RSD(%)	Repeatability RSD(%)	Stability RSD(%)	Average Recovery(%)	Recov-Recovery RSD(%)
Total flavonoids	Rutin	y = 10.037x + 0.0022	0.9992	1.11	1.14	2.15	100.23	1.36
Total polysaccharides	Anhydrous glucose	y = 40.754x + 0.013	0.9991	0.37	1.98	2.03	99.34	1.87
Total saponins	Platycodin D	y = 2.7929x + 0.0671	0.9993	2.28	1.41	2.10	99.36	1.95
Total saponins	Licoric acid	y = 1E+06x + 18292	0.9996	1.98	1.85	1.70	99.80	2.07

3.1.2 Results of Total Flavonoid and Total Polysaccharide Content Determination

Samples of total flavonoids and total polysaccharides from three batches of Platycodon Decoction were processed according to the optimal purification protocol and then analyzed using UV spectroscopy. The total flavonoid content was calculated using rutin as the reference standard, and the total polysaccharide content was calculated using anhydrous glucose as the reference standard. The results showed that, after purification, the average total flavonoid content of Platycodon Decoction was 834 ± 12.51 mg/g, and the average total polysaccharide content was 120.8 ± 9.06 mg/g (Table 4). The total flavonoid content met the standard specified in the Chinese Pharmacopoeia* (30), which requires a total flavonoid content of not less than 80% (calculated as rutin).

Table 4 Results of total flavonoid and total polysaccharide content analysis for three batches of Jiegeng Decoction (Mean ± SD, n=3).

Batch	Total Flavonoid Content (mg/g)	Total Polysaccharide Content (mg/g)
1	825.6	114.2
2	838.2	122.5
3	838.2	125.7
Average	834±12.51	120.8±9.06
RSD（%）	1.50	7.50

3.1.3 Results of Total Saponin Content Determination

The HPLC method was used to determine the content of Platycodin D and glycyrrhizic acid in the total saponins of Platycodon Decoction. Chromatograms of the reference standards and test sample solutions showed consistent peaks at the same retention times (Figure 1). Calculations based on the standard curve showed that the average content of Platycodin D in the three batches of samples was 31.8 ± 0.5 mg/g, and the average content of glycyrrhizic acid was 8.985 ± 0.205 mg/g (Table 5), which met the standards specified in the *Chinese Pharmacopoeia* (30), which stipulate that the content of Platycodin D must not be less than 0.10% and that of glycyrrhizic acid must not be less than 2.0%.

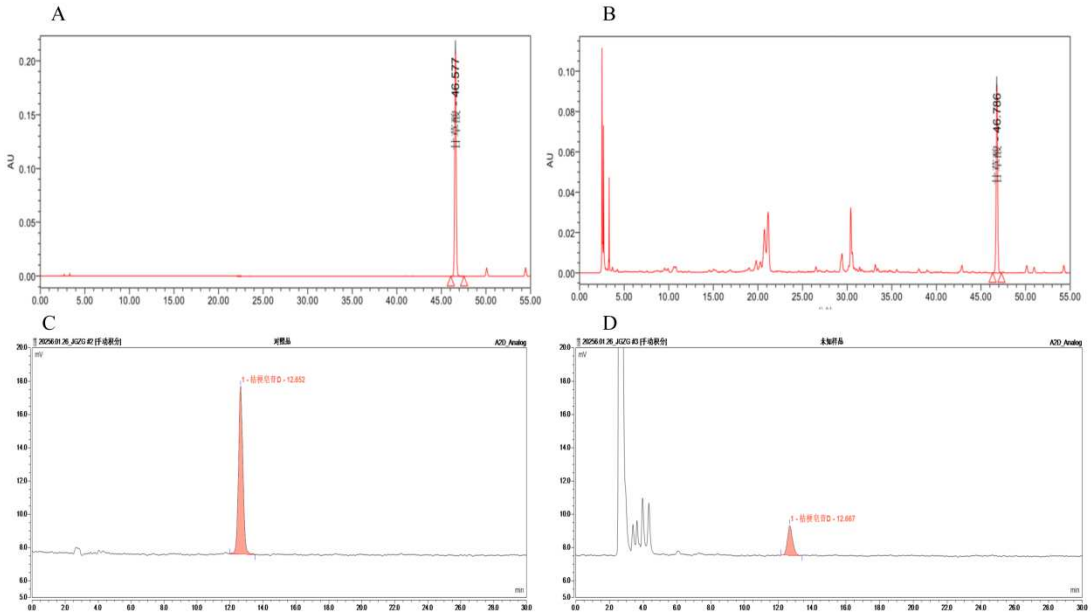


Fig. 1 HPLC chromatograms of platycodin D and glycyrrhizic acid in total saponins from Jiegeng Decoction. (A) Platycodin D reference standard (HPLC-ELSD); (B) Total saponins sample (HPLC-ELSD); (C) Glycyrrhizic acid reference standard (HPLC-PDA); (D) Total saponins sample (HPLC-PDA).

Table 5 Content determination results of platycodin D and glycyrrhizic acid in total saponins from three batches of Jiegeng Decoction (Mean ± SD, n=3).

Batch	Platycodin D Content (mg/g)	Glycyrrhizic Acid Content (mg/g)
1	31.5	8.85
2	32.1	9.10
3	31.8	9.00
Average	31.8±0.5	8.985±0.205
RSD (%)	1.57	2.28

3.2 Network Pharmacology Prediction Results

3.2.1 Screening Results for Active Ingredients and Target Molecules in Jiegeng Decoction

Using the TCMSP database and applying screening criteria of oral bioavailability (OB) ≥ 30% and drug-like score (DL) ≥ 0.18, 153 active ingredients in Jiegeng Decoction were identified, including 33 from Platycodon grandiflorus and 120 from Glycyrrhiza uralensis (36, 37). The 2D structures of these active components were imported into the Swiss Target Prediction Database to predict the corresponding targets. After merging the results and removing the duplicates, 370 potential targets were identified.

3.2.2 Results of Screening for Drug-Resistant Lung Cancer-Related Targets and Overlapping Targets

A search of the Genecards database using the keyword “Drug-resistant lung cancer” yielded 2,823 drug-resistant lung cancer-related target genes (38). By intersecting the 370 potential targets of the active components in the Jiegeng Decoction with 2,823 drug-resistant lung cancer-related targets, 157 common targets were identified (Figure 2). These common targets are considered potential mechanisms through which the Jiegeng Decoction reverses drug resistance in lung cancer.

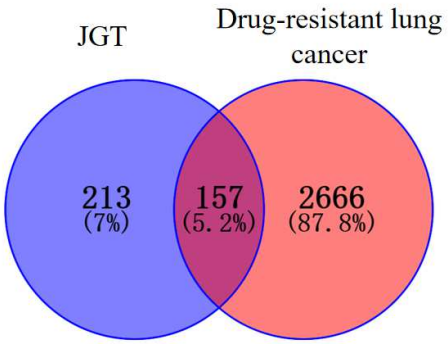


Fig. 2 Venn diagram of overlapping targets between Jiegeng Decoction and drug-resistant lung cancer.

3.2.3 Results of the "Active Ingredient–Disease Target" Network Analysis

The 157 overlapping targets and their corresponding active ingredients were imported into Cytoscape 3.10.1 to construct a "Traditional Chinese Medicine Active Ingredients–Disease Targets" network diagram (Figure 3). Network topology analysis revealed that the top ten core active ingredients were liquiritin, isoliquiritin, glycyrrhizic acid, Platycodin A D, platycodin A (platycodin A), 1-methoxyphaseollidin, platycoside E (Platyeoside E), licochalcone A, polygalacin D, and glabrene. Glycyrrhizin, isoglycyrrhizin, glycyrrhetic acid, and platycodin D are the marker components used to evaluate the quality of Platycodon Decoction in the *Chinese Pharmacopoeia* (30) and have been identified as the core active ingredients for subsequent molecular docking validation.

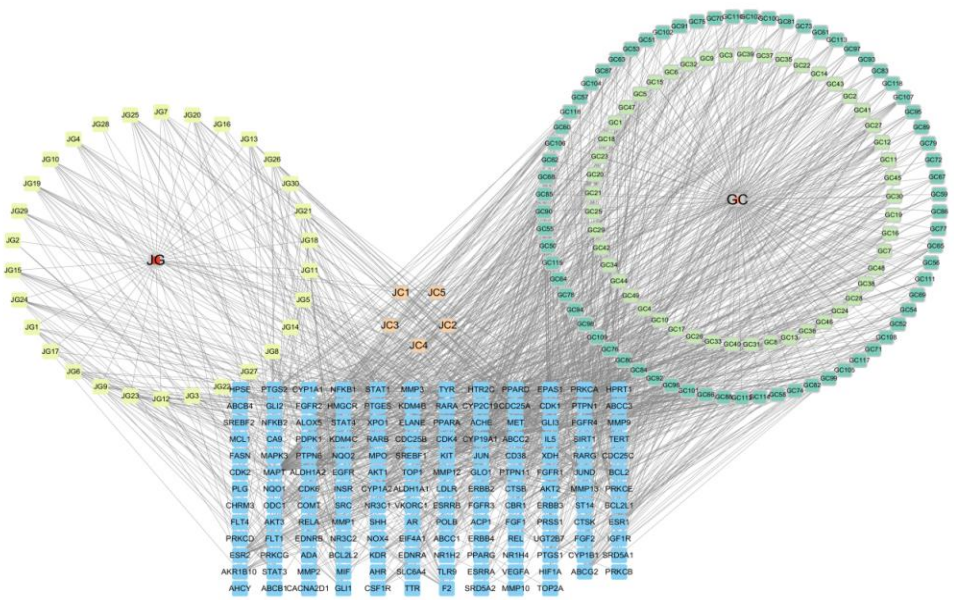
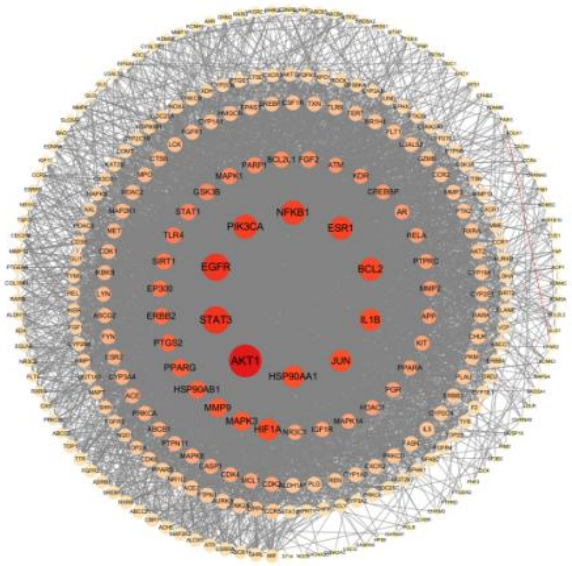


Fig. 3 Network of active components of Jiegeng Decoction and drug-resistant lung cancer targets. Nodes represent compounds (diamonds) and targets (circles), with node size proportional to degree centrality.

3.2.4 Results of Protein-Protein Interaction (PPI) Network Analysis

The 157 overlapping targets were imported into the STRING database to construct a PPI network, which was then visualized and analyzed topologically using Cytoscape 3.10.1 software (Figure 4) (38). Sorted by degree centrality (DC), the top ten targets by degree were phosphatidylinositol-4,5-bisphosphate 3-kinase catalytic subunit α (PIK3CA), serine/threonine protein kinase 1 (AKT1), epidermal growth factor receptor (EGFR), nuclear factor κB subunit 1 (NFKB1), signal transduction and transcription activator 3 (STAT3), Jun proto-oncogene (JUN), interleukin-1β (IL1B), estrogen receptor 1 (ESR1), B-cell lymphoma 2 (BCL2), and heat shock protein 90α family class A member 1 (HSP90AA1). The above targets were identified as core targets; among them, PIK3CA, AKT1, and NFKB1 were directly related to the PI3K/AKT/NF-κB signaling pathway and thus became the focus of subsequent experimental validation.



508

Fig. 4 PPI network of overlapping targets. Nodes represent targets, with node size and color intensity proportional to degree centrality. 509 510

3.2.5 Results of GO Functional Enrichment and KEGG Pathway Enrichment Analyses 511

GO functional enrichment and KEGG pathway enrichment analyses were performed on 157 overlapping targets using the Metascape platform, with a significance threshold of $P < 0.05$ (37). GO analysis yielded 912 biological process (BP) entries, 91 cellular component (CC) entries, and 180 molecular function (MF) entries. In terms of the number of enriched entries, BPs accounted for the highest proportion, followed by MFs, whereas CCs were relatively fewer. KEGG enrichment analysis identified 181 signaling pathways. We selected the top 10 most significant entries from the GO analysis to create a bar chart, and the top 20 most significant pathways from the KEGG analysis to create a bubble chart. 512 513 514 515 516 517 518 519

The GO functional enrichment analysis (Figure 5) showed that BPs were primarily enriched in negative regulation of the apoptotic process, signal transduction, and positive regulation of transcription by RNA polymerase II; CC was primarily distributed in the cytoplasm, plasma membrane, and cytosol; MF was predominantly associated with protein binding, identical protein binding, and ATP binding. These results suggest that overlapping targets may be involved in key biological processes such as cell survival, signal transduction, and transcriptional regulation. 520 521 522 523 524 525 526

KEGG pathway enrichment analysis (Figure 5) showed that the main signaling pathways involved in the reversal of drug resistance in lung cancer by Jiegeng Decoction include the phosphoinositide-3-kinase/ phosphatidylinositol-3-kinase/serine/threonine kinase (PI3K-Akt) signaling pathway, the nuclear factor κB (NF-κB) signaling pathway, the Janus kinase/signal transduction and transcription activator (JAK-STAT) signaling pathway, the mitogen-activated protein kinase (MAPK) signaling pathway, and the calcium signaling pathway, among others. Among these, the PI3K-Akt signaling pathway showed the highest enrichment (the highest number of genes and the largest -log10(P-value)), suggesting that this pathway is the core pathway through which Jiegeng Decoction reverses drug resistance in lung cancer. The NF- 527 528 529 530 531 532 533 534 535

κB signaling pathway was also significantly enriched, and together with the PI3K-Akt signaling pathway, they formed the PI3K/AKT/NF-κB signaling axis. These predictive results provide a clear theoretical basis for subsequent in vitro validation.

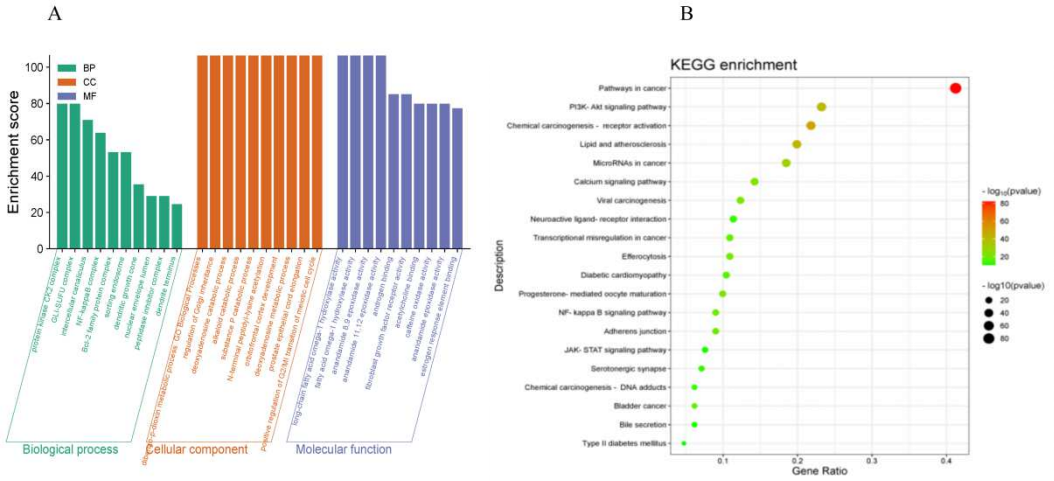


Fig. 5 GO functional enrichment (A) and KEGG pathway(40-42) enrichment (B) analysis of Jiegeng Decoction in reversing drug-resistant lung cancer.

3.2.6 Results of Molecular Docking Validation

To validate the reliability of the network pharmacology predictions, the core active components (platycodin D, glycyrrhizin, isoglycyrrhizin, and glycyrrhetic acid) were selected for molecular docking validation with core targets (PIK3CA, AKT1, and NF-κB1) (38, 39). The docking results showed that the binding energies for all ligand-receptor pairs were less than −5.0 kcal/mol (Table 6), indicating that both the core active components and the core targets exhibit good binding activity. Among them, Platycodin D had the lowest binding energy with PIK3CA (−9.6 kcal/mol), demonstrating the strongest binding affinity.

Table 6 Molecular docking binding energies of core active components from Jiegeng Decoction with core targets (kcal/mol).

Active Ingredient	PIK3CA Binding Energy (kcal/mol)	NF-κB Binding Energy (kcal/mol)	AKT1 Binding Energy (kcal/mol)
Platycodin D	-9.6	-8.6	-9.1
Glycyrrhizin	-5.9	-7.4	-6.5
Isoglycyrrhizin	-6.3	-6.2	-7.0
Glycyrrhetic acid	-8.5	-7.5	-8.3

PyMOL software was used to generate docking models (Figure 6) and analyze the interaction patterns between the active compound and the target protein. The results showed that the binding of Platycodin D to PIK3CA involves amino acid residues such as ASN-47, TYR-263, and LEU-44, forming stable interactions via hydrogen bonds, binding sites with NF-κB including VAL-114 and TYR-46, and binding to AKT1 occurs via SER-51, SER-74, and SER-

80. The interactions of glycyrrhizin with PIK3CA, NF-κB, and AKT1 involved residues SER-212, SER-242, and VAL-270, respectively. Docking studies of isoglycyrrhizin and glycyrrhetic acid with the aforementioned targets revealed similar hydrogen-bond networks. These results indicate that Platycodin D, glycyrrhizin, isoglycyrrhizin, and glycyrrhetic acid can stably interact with the target proteins PIK3CA, NF-κB, and AKT1, suggesting that these active components may reverse drug resistance by regulating the PI3K/AKT/NF-κB pathway.

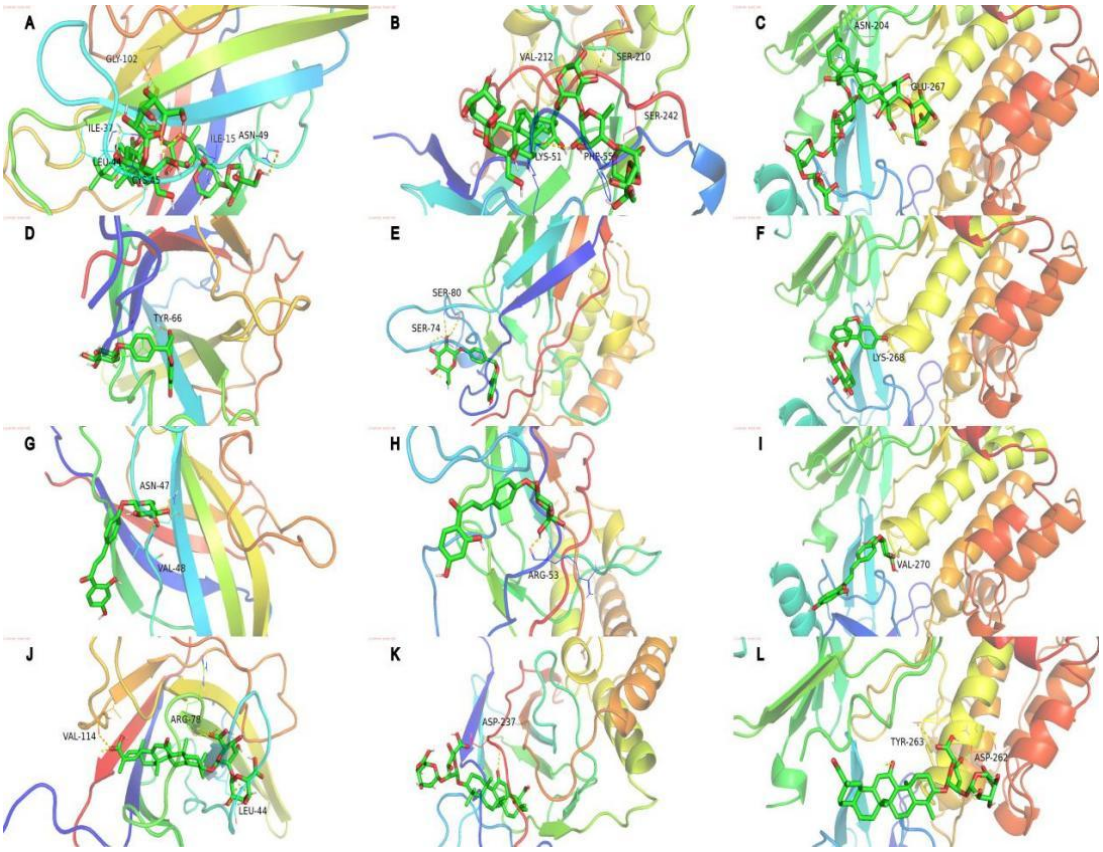


Fig. 6 Molecular docking models of core active components with core targets. (A) Platycodin D-PIK3CA; (B) Platycodin D-NF-κB; (C) Platycodin D-AKT1; (D) Liquiritin-PIK3CA; (E) Liquiritin-NF-κB; (F) Liquiritin-AKT1; (G) Isoliquiritin-PIK3CA; (H) Isoliquiritin-NF-κB; (I) Isoliquiritin-AKT1; (J) Glycyrrhizic acid-PIK3CA; (K) Glycyrrhizic acid-NF-κB; (L) Glycyrrhizic acid-AKT1. Hydrogen bonds are shown as yellow dashed lines.

In summary, network pharmacology predictions indicated that Jiegeng Decoction exerts its effects through 153 active components and 157 potential targets. Its core active components are glycyrrhizin, isoglycyrrhizin, glycyrrhetic acid, and platycodon saponin D. The core targets were PIK3CA, AKT1, and NF-κB1, with enrichment primarily observed in the PI3K-Akt and NF-κB signaling pathways. Molecular docking confirmed that the core constituents exhibited strong binding affinity for the core targets. Based on the above results combined with PPI key target analysis and literature reports (22, 23), the PI3K/AKT/NF-κB signaling pathway has been identified as the core pathway through which Jiegeng Decoction reverses cisplatin resistance in lung cancer. Subsequent in vitro cellular experiments will focus on this pathway for validation studies.

3.3 Effects of the Components of Jiegeng Decoction on Cell Proliferation and Cisplatin Sensitivity

3.3.1 Effects of Three Categories of Components in Jiegeng Decoction on the Activity of A549 and A549/DDP Cells

The CCK-8 assay was used to evaluate the cytotoxic effects of total polysaccharides (PPG), total flavonoids (FPG), and total saponins (SPG) from Platycodon Decoction on A549 human lung cancer cells and A549/DDP cisplatin-resistant lung cancer cells. After treating both cell lines with different concentrations of PPG, FPG, and SPG (0.1, 0.2, 0.3, 0.4, 0.5, 0.6 mg/mL) for 24 h, the cell viability was measured (32).

The results showed (Fig. 7A, Fig. 7B) that within the concentration range of 0.1–0.6 mg/mL, the three components of Jiegeng Decoction exhibited concentration-dependent inhibition of the viability of both A549 and A549/DDP cells as the administered concentration increased. Compared with A549/DDP cells, the same concentrations of Jiegeng Decoction components exhibited a stronger inhibitory effect on A549 cells. Among the three components, SPG at the same concentration exhibited the strongest inhibitory effect on both cell types, followed by FPG, whereas PPG showed a relatively weaker effect. It is worth noting that when the concentrations of the components of the Jiegeng Decoction were below 0.3 mg/mL, no significant cytotoxic effects were observed in either cell line (cell survival rate > 90%). Therefore, to rule out the interference of direct cytotoxicity by the drugs on the results of subsequent mechanistic studies, 0.1 mg/mL was selected as the concentration of the components of the Jiegeng Decoction in subsequent migration, apoptosis, and western blot experiments.

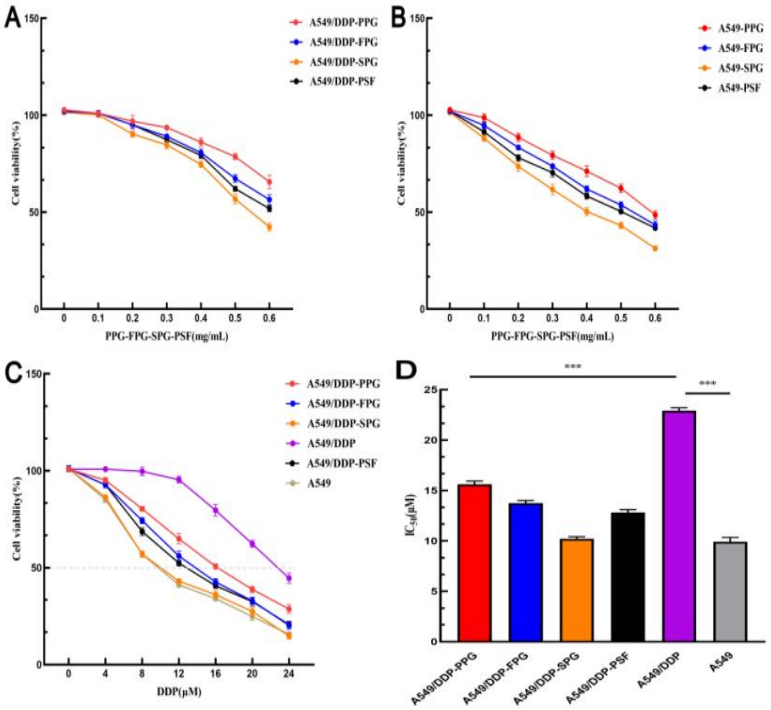


Fig.7 Effects of three components of Jiegeng Decoction, cisplatin and their combination on cell viability.compared with the control group .(A) Cytotoxicity of PPG, FPG and SPG on A549/DDP cells; (B) Cytotoxicity of PPG, FPG and SPG on A549 cells; (C) Cytotoxic effects

of DDP alone and DDP combined with PPG, FPG or SPG on A549/DDP cells; (D) Comparison of IC_{50} values of DDP in A549 vs. A549/DDP cells, and IC_{50} values of DDP alone vs. DDP combined with PPG, FPG or SPG in A549/DDP cells ($P < 0.001$ vs. A549 group; $P < 0.001$ vs. DDP alone group). Data are presented as Mean ± SD (n=3).

3.3.2 Effects of Cisplatin on the Viability of A549 and A549/DDP Cells and Verification of Drug Resistance

The CCK-8 assay was used to assess the effects of different cisplatin concentrations (4, 8, 12, 16, 20, and 24 μM) on the viability of A549 and A549/DDP cells. The results showed (Figure 7C) that as the concentration of cisplatin increased, the viability of both A549 and A549/DDP cells gradually decreased in a concentration-dependent manner. However, A549/DDP cells required higher concentrations of cisplatin to achieve an inhibitory effect comparable to that observed in the A549 cells. Calculations showed that the half-maximal inhibitory concentration (IC_{50}) of cisplatin for A549 cells was 9.92 ± 0.42 μM, while the IC_{50} for A549/DDP cells was 22.91 ± 0.29 μM (Figure 7D). The resistance index (RI = IC_{50}(A549/DDP) / IC_{50}(A549)) was approximately 2.31, indicating that A549/DDP cells possess stable cisplatin resistance and can be used in subsequent drug resistance reversal experiments.

3.3.3 Effect of Combining Three Components of Jiegeng Decoction with Cisplatin on Restoring Cisplatin Sensitivity in A549/DDP Cells

To evaluate the sensitizing effects of the three components of Jiegeng Decoction on cisplatin, A549/DDP cells were treated with 0.1 mg/mL PPG, FPG, and SPG, respectively, in combination with different concentrations of cisplatin (4, 8, 12, 16, 20, and 24 μM) for 24 h. Cell viability was measured, and the cisplatin IC_{50} was calculated [26]. The results showed (Fig. 7C and Fig. 7D) that compared with the cisplatin monotherapy group, the combination of cisplatin with PPG, FPG, and SPG exhibited stronger cytotoxic effects on A549/DDP cells, with more pronounced inhibition of cell viability. Calculations revealed that the IC_{50} of the cisplatin monotherapy group was 22.91 ± 0.29 μM; when combined with PPG, the IC_{50} of cisplatin decreased to 15.61 ± 0.33 μM; when combined with FPG, the IC_{50} of cisplatin decreased to 13.75 ± 0.25 μM; and when combined with SPG, the IC_{50} of cisplatin decreased to 10.21 ± 0.20 μM (Table 7). Among these, the IC_{50} value in the SPG combination group was closest to that of A549 cells (9.92 ± 0.42 μM), indicating that SPG exhibited the most pronounced sensitizing effect. The sensitizing effects of the three components were ranked as SPG > FPG > PPG.

Table 7 Effects of three components of Jiegeng Decoction combined with cisplatin on the IC_{50} of cisplatin in A549/DDP cells (Mean ± SD, n=3). Reversal fold = IC_{50}(DDP alone) / IC_{50}(DDP + component).

Group	IC_{50}（μM）	ReversalFactor
DDP alone	22.91±0.29	-
DDP + PPG	15.61±0.33	1.47
DDP + FPG	13.75±0.25	1.67

DDP + SPG	10.21±0.20	2.24

3.4 Results of the Cell Scratch Assay

To investigate the effects of total polysaccharides (PPG), total flavonoids (FPG), and total saponins (SPG) from Jiegeng Decoction, either alone or in combination with cisplatin, on the migratory capacity of A549/DDP cells, a cell scratch assay was performed (32). The experimental groups were as follows: control group (Control), cisplatin group (DDP, 20 μM), PPG group (0.1 mg/mL), FPG group (0.1 mg/mL), SPG group (0.1 mg/mL), DDP+PPG group, DDP+FPG group, DDP+SPG group, and DDP+PSF group. Photographs were taken at 0, 24, and 48 h after the scratch was made, and the cell migration rates were calculated. To eliminate the interference of cell proliferation on the migration results, the cells were cultured in serum-free medium after scratching.

3.4.1 Inhibitory Effects of the Three Components of Jiegeng Decoction on A549/DDP Cell Migration When Used Alone

The results show (Figs. 8 and 9) that, compared with the control group, treatment of A549/DDP cells with PPG, FPG, or SPG alone for 24 h and 48 h significantly inhibited cell migration ($P < 0.01$ or $P < 0.001$). At the 24-hour time point, the cell migration rate in the control group was 38.52 ± 2.13%, while the migration rates in the PPG, FPG, and SPG groups decreased to 28.34 ± 1.89%, 24.16 ± 1.52%, and 20.08 ± 1.36%, respectively. At the 48-hour time point, the cell migration rate in the control group was 67.43 ± 2.56%, while the migration rates in the PPG, FPG, and SPG groups decreased to 51.27 ± 2.01%, 44.83 ± 1.78%, and 37.62 ± 1.95%, respectively. Among the three components, SPG exhibited the strongest inhibitory effect on cell migration, followed by FPG, whereas PPG had a relatively weaker effect, consistent with the trends observed in the CCK-8 results.

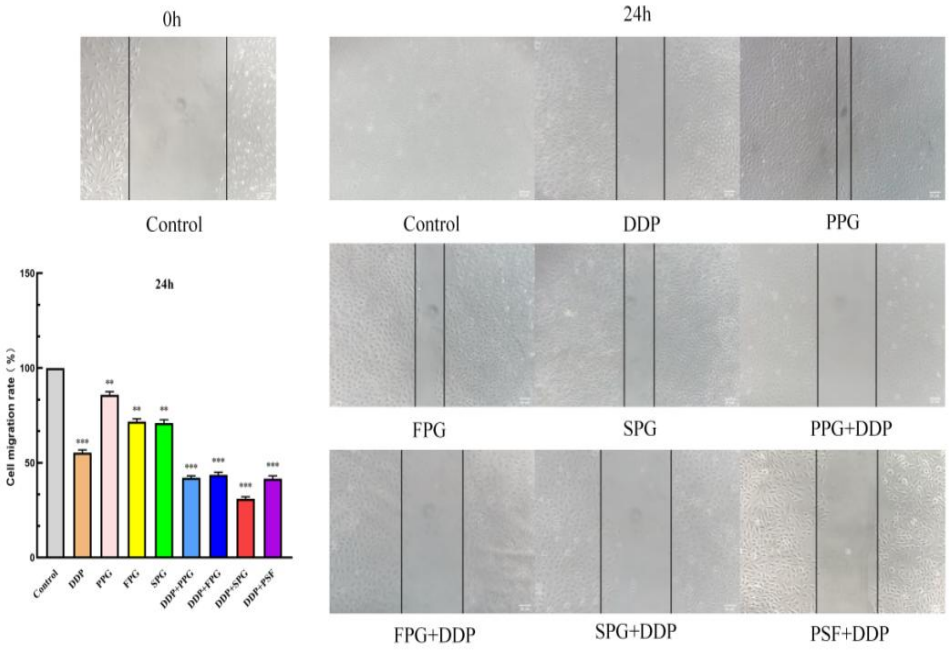


Fig. 8 Effects of active components of Platycodon grandiflorus decoction and combined medication on cell migration ability at 0 h and 24 h.

Note: Cell migration was assessed using a wound healing assay. Compared with the control group, PPG, FPG, SPG, and their combinations with DDP inhibited cell migration to varying degrees at 24 h. Data are presented as the percentage of wound closure relative to 0 h (set as 100%). (Ctrl, control; DDP, cisplatin; PPG, platycodin D; FPG, flaxseed polysaccharide; SPG, saponin; PSF, polysaccharide fraction). Data are presented as mean ± SD (n=3).

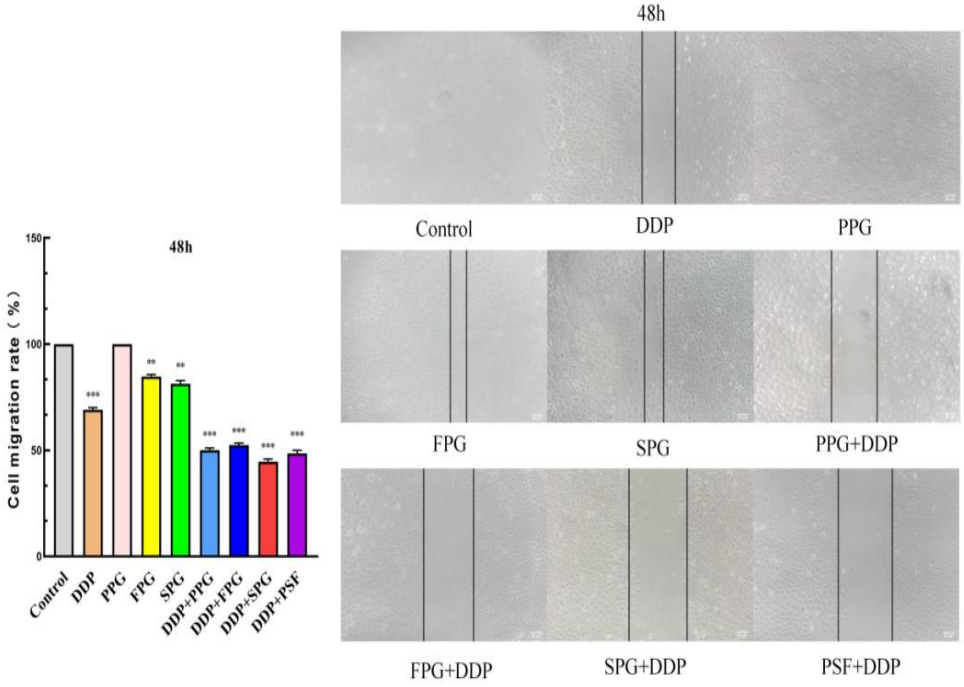


Fig. 9 Effects of active components of Platycodon grandiflorus decoction and combined medication on cell migration ability at 48 h.

Note: Cell migration was assessed using a wound healing assay. Compared with the control group, treatment with DDP, PPG, FPG, SPG, PSF, or their combinations with DDP significantly inhibited cell migration at 48 h. The cell migration rate was calculated as the percentage of wound closure at 48 h relative to the initial wound area at 0 h. Data are presented as mean ± SD (n=3). *P < 0.05, **P < 0.01, ***P < 0.001 vs. control group; *P < 0.05, **P < 0.01, ***P < 0.001 vs. DDP alone group. (Ctrl, control; DDP, cisplatin; PPG, platycodin D; FPG, flaxseed polysaccharide; SPG, saponin; PSF, polysaccharide fraction).

3.4.2 Inhibitory Effects of Three Categories of Components from Jiegeng Decoction Combined with Cisplatin on the Migration of A549/DDP Cells

The results showed (Figs. 8 and 9) that compared with the cisplatin monotherapy group, the cell migration capacity of A549/DDP cells was significantly inhibited (P < 0.001) 24 h and 48 h after treatment with cisplatin in combination with PPG, FPG, and SPG. At the 24-hour time point, the cell migration rate in the cisplatin monotherapy group was 31.45 ± 1.67%,

whereas the migration rates in the DDP+PPG, DDP+FPG, and DDP+SPG groups decreased to 22.67 ± 1.45%, 18.93 ± 1.28%, and 14.26 ± 1.07%, respectively. At the 48-hour time point, the cell migration rate in the cisplatin monotherapy group was 59.38 ± 2.23%, while the migration rates in the DDP+PPG, DDP+FPG, and DDP+SPG groups decreased to 43.16 ± 1.89%, 36.52 ± 1.64%, and 28.74 ± 1.58%, respectively. In the DDP+PSF group (combination of the three components with cisplatin), the migration rate at the 48-hour time point decreased to 26.31 ± 1.52%, showing no significant difference compared to the DDP+SPG group, indicating that SPG plays a dominant role in inhibiting migration. The above results indicate that the three components of the Jiegeng Decoction, whether used alone or in combination with cisplatin, can significantly inhibit the migration capacity of A549/DDP cells, with SPG exhibiting the most pronounced inhibitory effect, which was further enhanced when combined with cisplatin.

3.5 Induction of Cell Apoptosis by Components of Platycodon Decoction

To investigate the apoptotic effects of total polysaccharides (PPG), total flavonoids (FPG), and total saponins (SPG) from Platycodon Decoction, either alone or in combination with cisplatin, on A549/DDP cells, Annexin V-FITC/PI double-staining flow cytometry was employed for evaluation (32). The experimental groups were the same as those described in Section 3.4. Cells were harvested for analysis 48 h after drug treatment. Cells positive for Annexin V-FITC alone were classified as early apoptotic cells, cells positive for PI alone were classified as late apoptotic or necrotic cells, double-positive cells were classified as late apoptotic cells, and double-negative cells were classified as viable cells. The total apoptosis rate was calculated as the sum of early and late apoptosis rates.

3.5.1 Effects of Three Components of Jiegeng Decoction Administered Alone on Apoptosis in A549/DDP Cells

The results showed (Figure 10) that the spontaneous apoptosis rate of A549/DDP cells in the control group was 5.75 ± 0.60%. Compared to the control group, treatment with PPG, FPG, or SPG alone for 48 h induced apoptosis ($P < 0.05$). Specifically, the apoptosis rates in the PPG group were 8.75 ± 0.67%, in the FPG group 12.52 ± 0.50%, and in the SPG group 18.39 ± 1.00%, respectively. Among the three components, SPG induced the strongest apoptosis, followed by FPG, whereas PPG had a relatively weaker effect, consistent with the trends observed in the CCK-8 and scratch assay results. The apoptosis rate in the cisplatin monotherapy group (DDP, 20 μM) was 21.45 ± 1.53% ($P < 0.01$ vs. the control group), which was slightly higher than that in the SPG monotherapy group.

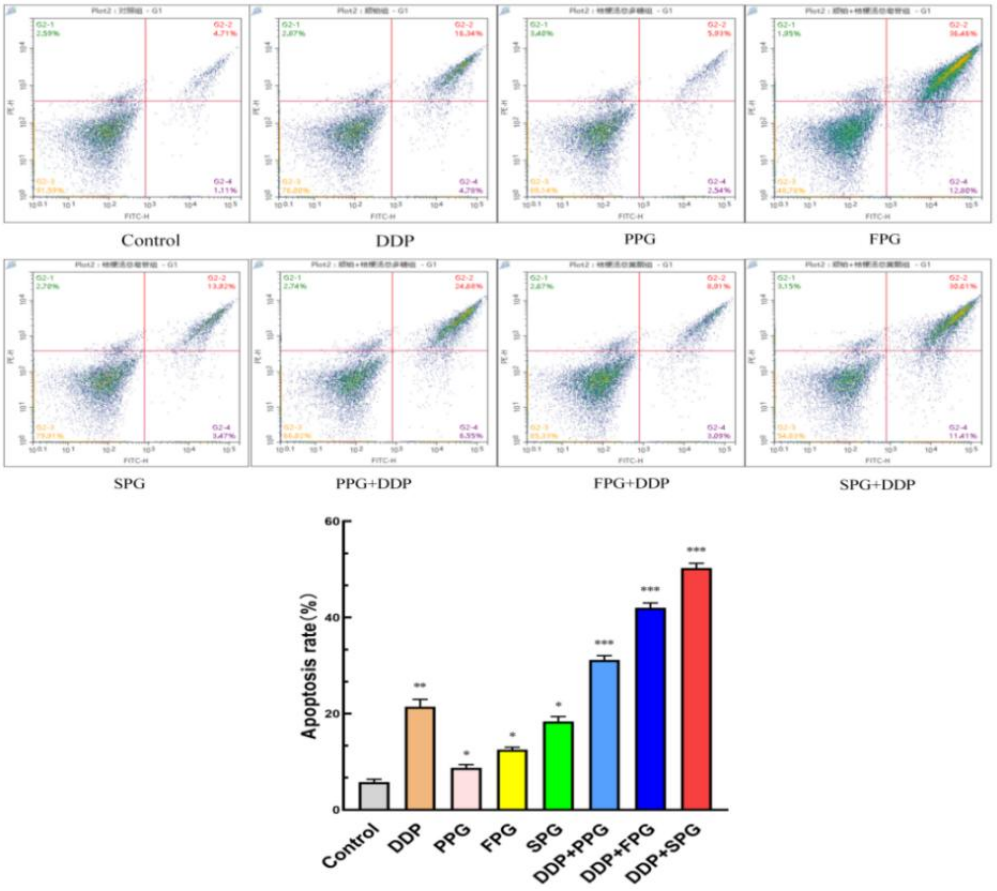


Fig.10 Induction of apoptosis by active components of Platycodon grandiflorus decoction and combined medication.

Note: Apoptosis was detected by flow cytometry after Annexin V-FITC/PI double staining. Compared to the control group (apoptosis rate: 2.39%), treatment with DDP (4.71%), PPG (2.87%), FPG (16.34%), SPG, and their combinations induced apoptosis to varying degrees. The combinations of FPG+DDP (5.82%), FPG+PPG (1.35%), FPG+FPG+DDP (1.26%), and FPG+FPG+DDP+PPG (1.41%) also showed pro-apoptotic effects. Data are presented as mean ± SD (n=3).

3.5.2 Synergistic Effect of Three Categories of Platycodon Decoction Components Combined with Cisplatin on Apoptosis in A549/DDP Cells

The results showed (Figure 10) that compared with the cisplatin monotherapy group, the apoptosis rates of A549/DDP cells were significantly increased ($P < 0.001$) following treatment with cisplatin in combination with PPG, FPG, and SPG. The apoptosis rate in the DDP+PPG, DDP+FPG, and DDP+SPG groups rose to 31.16 ± 0.90%, in the DDP+FPG group to 42.02 ± 1.98%, and in the DDP+SPG group to 50.26 ± 1.33%, respectively. The apoptosis rate in the DDP+PSF group (cisplatin combined with the three components) was 51.48 ± 1.45%, showing no significant difference compared to the DDP+SPG group, indicating that SPG plays a dominant role in inducing apoptosis.

Jin's formula was used to evaluate the synergistic effects of the combination therapy: $q = E(A + B) / (EA + EB - EA \times EB)$, where $q > 1.15$ indicates a synergistic effect, $q = 0.85–1.15$ indicates an additive effect, and $q < 0.85$ indicates an antagonistic effect (43). The calculation

results showed that the q-value for the combination of SPG and cisplatin was 1.38, demonstrating the strongest synergistic pro-apoptotic effect; the q-value for the combination of FPG and cisplatin was 1.21, also exhibiting a synergistic effect; and the q-value for the combination of PPG and cisplatin was 1.08, primarily showing an additive effect. These results indicate that all three components of the Jiegeng Decoction can induce apoptosis in A549/DDP cells, and their combination with cisplatin further enhanced the apoptotic effect. SPG exhibited the strongest synergistic pro-apoptotic effect with cisplatin, increasing the apoptosis rate from 21.45% with cisplatin alone to 50.26%, a 2.34-fold increase.

3.6 Results of Western blot analysis of protein expression in the PI3K/AKT/NF-κB pathway

To verify whether total polysaccharides (PPG), total flavonoids (FPG), and total saponins (SPG) from Jiegeng Decoction, either alone or in combination with cisplatin, reverse cisplatin resistance in A549/DDP cells by inhibiting the PI3K/AKT/NF-κB signaling pathway, western blotting was used to detect the expression levels of PI3K, AKT, p-AKT (Ser473), and NF-κB p65 protein expression levels in each cell group (32). β-actin was used as an internal control for normalization, and the relative expression level of each protein and the p-AKT/AKT ratio were calculated.

The results showed (Figure 11) that, compared with the control group, the expression levels of PI3K, p-AKT, NF-κB, and p-AKT/AKT ratios were all reduced; the inhibitory effect was most pronounced in the cisplatin group, followed by the total saponins and total flavonoids groups; the total polysaccharide group also exhibited an inhibitory effect (**$P < 0.01$ or ***$P < 0.001$). There were no significant changes in total AKT protein expression across all groups, suggesting that the Jiegeng Decoction primarily affects AKT phosphorylation levels. Compared with the control group, the expression of PI3K, p-AKT, and NF-κB, as well as the p-AKT/AKT ratio, was significantly reduced in all combination therapy groups. The reduction was most pronounced in the cisplatin + total saponins and cisplatin + total flavonoid groups, and the cisplatin + total polysaccharide group also showed a significant reduction (***$P < 0.001$ or **** $P < 0.0001$). This indicates that the combination of any of the three components of the Jiegeng Decoction with cisplatin significantly enhanced the inhibitory effect on the PI3K/AKT/NF-κB pathway, with the synergistic effect of total saponins and total flavonoids being the most pronounced.

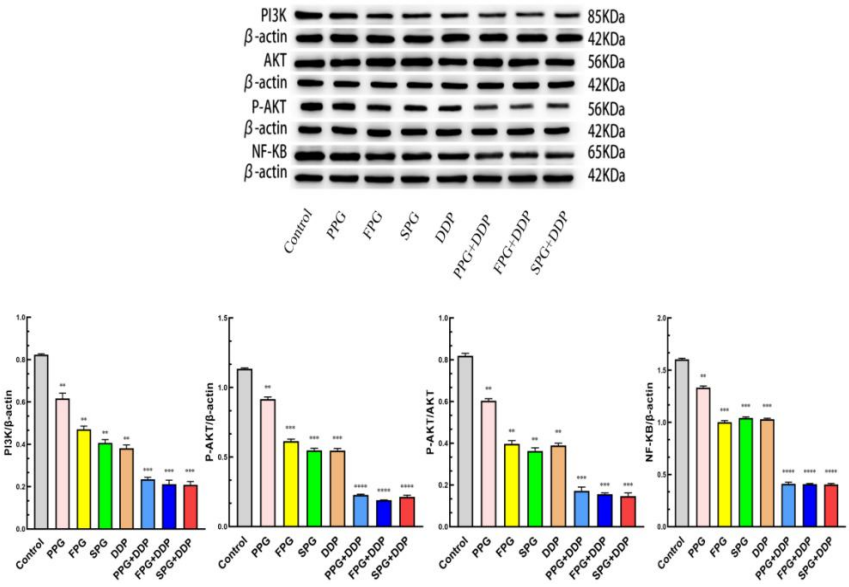


Fig. 11 Effects of pharmacodynamic components of Platycodon grandiflorus decoction and combined medication on the expression of PI3K/AKT/NF-κB pathway-related proteins.

Note: Protein expression levels of PI3K (85 kDa), AKT (56 kDa), p-AKT (56 kDa), and NF-κB (65 kDa) were detected using western blotting, with β-actin (42 kDa) serving as the loading control. Compared to the control group, treatment with PPG, FPG, SPG, DDP, and their combinations differentially regulated the expression of these pathway proteins. The quantification of relative protein expression (normalized to β-actin) is shown in the bar graphs below each blot. Data are presented as mean ± SD (n=3).

4. Discussion

This study is the first to systematically compare the differences in the efficacy of three types of constituents—total flavonoids, polysaccharides, and saponins—in Jiegeng Decoction for reversing cisplatin resistance. The results show that all three types of constituents exhibit sensitizing activity to varying degrees, with potency ranked as follows: total saponins > total flavonoids > total polysaccharides. This ranking does not correlate simply with the content measurements of the three components (total saponins: 31.8 ± 0.5 mg/g of Platycodin D; total flavonoids: 834 ± 12.51 mg/g; total polysaccharides: 120.8 ± 9.06 mg/g) is not a simple positive correlation, suggesting that the differences in sensitization activity may stem from variations in the targeting ability and bioavailability of the active components. Total saponins exhibit the optimal sensitizing effect because of the following two factors. First, Platycodin D, as the primary active component in total saponins, demonstrated the strongest binding affinity for PIK3CA, AKT1, and NF-κB1 (binding energies of −9.6, −9.1, and −8.6 kcal/mol, respectively), significantly outperforming the flavonoid components (glycyrrhizin and isoglycyrrhizin) (38, 39). Furthermore, it has been reported that Platycodin D can regulate tumor drug resistance through multiple pathways, including inhibition of the Nrf2/ARE pathway to reverse cisplatin resistance and downregulation of MMP-2/9 expression to suppress invasion and metastasis (32, 43, 44). Although the binding activity of glycyrrhizin, isoglycyrrhizin, and glycyrrhetic acid in total flavonoids is slightly lower, they can enhance the overall therapeutic effect through synergistic interactions among multiple components (13, 14, 45). The sensitizing effect of total polysaccharides is relatively weak, primarily manifesting as an additive effect,

which may be related to the fact that polysaccharide components exert their effects indirectly, mainly through immune modulation (46).

Abnormal activation of the PI3K/AKT signaling pathway is one of the key molecular mechanisms underlying chemotherapy resistance in tumors (47). Under normal conditions, PI3K is activated by phosphorylation by receptor tyrosine kinases (RTKs), which in turn catalyze the conversion of PIP2 to PIP3, transiently activate AKT, and promote cell proliferation and survival through downstream signaling pathways such as NF-κB. However, in tumor cells, mutations in the PIK3CA gene, loss of the PTEN gene, or overexpression of the AKT gene can lead to sustained activation of this pathway, thereby promoting cell proliferation, invasion, and metastasis, resulting in chemoresistance (47, 48). Western blotting results from this study showed that the expression levels of PI3K, p-AKT, and NF-κB p65 proteins in A549/DDP cells were higher than those in A549 cells (control group data), confirming that the PI3K/AKT/NF-κB pathway is abnormally activated in drug-resistant cells, consistent with previous reports (22, 23). This study found that each of the three components of the Jiegeng Decoction, when used alone, could downregulate the expression of PI3K, p-AKT, and NF-κB p65 proteins to varying degrees and reduce the p-AKT/AKT ratio, which was further enhanced when combined with cisplatin. It is worth noting that there were no significant changes in total AKT protein expression levels across all groups, suggesting that the Jiegeng Decoction primarily affects the phosphorylation and activation of AKT rather than the synthesis or degradation of AKT protein. This finding is highly consistent with the core targets predicted by network pharmacology (PIK3CA, AKT1, NFKB1), validating that the PI3K/AKT/NF-κB pathway is the core target pathway through which the Jiegeng Decoction reverses drug resistance (37-39). As a key downstream transcription factor in the PI3K/AKT pathway, NF-κB plays a crucial role in the development of drug resistance. Activated NF-κB can upregulate the expression of drug efflux pumps (such as P-gp, MRP1, and BCRP), accelerate drug efflux, simultaneously enhance the expression of anti-apoptotic genes (Bcl-2, XIAP), and suppress the expression of pro-apoptotic genes (Bax), thereby resisting chemotherapy-induced cell death (48). In this study, all three categories of components in the Jiegeng Decoction significantly downregulated NF-κB p65 protein expression, consistent with the downregulation trends observed for PI3K and p-AKT. This indicates that the Jiegeng Decoction restores the sensitivity of drug-resistant cells to cisplatin by inhibiting the overall activation of the PI3K/AKT/NF-κB signaling axis, thereby neutralizing the NF-κB-mediated drug resistance protection mechanism.

Through a research pathway of "network pharmacology prediction → molecular docking validation → in vitro experimental confirmation," this study systematically revealed the "multi-component–multi-target–multi-pathway" synergistic mechanism by which Jiegeng Decoction reverses drug resistance. Network pharmacology analysis revealed that the 153 active components of Jiegeng Decoction corresponded to 157 drug-resistance-related targets, primarily enriched in multiple signaling pathways such as PI3K-AKT, NF-κB, JAK-STAT, and MAPK (37-39). This study validated the PI3K/AKT/NF-κB pathway; however, whether other pathways (such as JAK-STAT and MAPK) are involved in the sensitizing effect of Jiegeng Decoction remains to be verified in subsequent experiments. From the perspective of multi-component synergy, Jiegeng saponin D, as the primary active component, plays a leading role in pathway inhibition, whereas flavonoids and triterpenoids, such as glycyrrhizic acid, glycyrrhizin, and isoglycyrrhizin, synergistically enhance the overall pharmacological efficacy through multi-target mechanisms (13, 14, 44-46). Previous studies have confirmed that glycyrrhizic acid can inhibit the proliferation and invasion of A549/DDP cells by regulating the JAK2/STAT3 pathway (45); liquiritin B, in combination with cisplatin, enhances antitumor activity and promotes apoptosis in A549 cells (14); and platycodon saponin D enhances the antitumor effect of cisplatin against A549 in situ transplanted tumors in nude mice (44). These studies provide supporting evidence for our findings and suggest that the Jiegeng Decoction

may involve a synergistic regulatory mechanism across multiple pathways and stages. From the perspective of Systemic Target-Oriented Diagnosis and Treatment" theory, this study embodies its core philosophy: guided by the holistic view of Traditional Chinese Medicine (TCM) and integrating modern biomedical findings, it adopts a strategy that combines macro- and micro-level approaches as well as target- and syndrome-oriented approaches to establish a diagnostic and therapeutic model that integrates disease-, syndrome-, and target-based approaches (26-28). Specifically, this study focuses on "disease differentiation" regarding cisplatin resistance in lung cancer, "syndrome differentiation" regarding the holistic regulatory effects of Jiegeng Decoction, and "target differentiation" regarding the core PIK3CA/AKT1/NF-κB1 targets. By leveraging the drug constituents to achieve systemic intervention across multiple targets and pathways, it enhances the specificity, efficacy, and safety of treatment. This research model provides a useful framework for the modernization of traditional Chinese herbal formulae (27).

In summary, based on the theory of "systematic identification of targets and targeted treatment," this study systematically elucidated the bioactive compounds and molecular mechanisms by which Jiegeng Decoction reverses cisplatin resistance in lung cancer through isolation and purification, network pharmacology predictions, and in vitro cellular experiments. This study confirmed that the three major components of Jiegeng Decoction—total flavonoids, total polysaccharides, and total saponins—can restore the sensitivity of A549/DDP cells to cisplatin by inhibiting the activation of the PI3K/AKT/NF-κB pathway, promoting apoptosis, and suppressing cell migration, with the synergistic effect of total saponins being the most pronounced. This study provides a scientific basis for the precise clinical application of Jiegeng Decoction and the development of novel chemotherapy sensitizers and serves as a model for modern research on traditional Chinese medicine formulas based on the theory of "systemic pattern differentiation and targeted treatment."

5. Conclusions

This study confirmed that three types of constituents in the Jiegeng Decoction—total flavonoids, total polysaccharides, and total saponins—can reverse cisplatin resistance in lung cancer cells by inhibiting the PI3K/AKT/NF-κB signaling pathway. CCK-8 results showed that, when the three types of components were used in combination with cisplatin, the cisplatin IC_{50} of A549/DDP cells decreased from 22.91 ± 0.29 μM to 15.61 ± 0.33 μM (total polysaccharides), 13.75 ± 0.25 μM (total flavonoids), and 10.21 ± 0.20 μM (total saponins), respectively. Cell scratch assays demonstrated that all three categories of compounds, either alone or in combination with cisplatin, significantly inhibited the migration of A549/DDP cells ($P < 0.01$ or $P < 0.001$). Flow cytometry results indicated that the apoptosis rate following the combination of the three components with cisplatin increased from 21.45 ± 1.53% with cisplatin alone to 31.16 ± 0.90% (total polysaccharides), 42.02 ± 1.98% (total flavonoids), and 50.26 ± 1.33% (total saponins). Western blot analysis confirmed that each of the three components, either alone or in combination with cisplatin, downregulated the expression of PI3K, p-AKT, and NF-κB proteins as well as the p-AKT/AKT ratio, and there was no significant change in total AKT protein expression. Taken together, these results indicate that the three components of Jiegeng Decoction restore the sensitivity of A549/DDP cells to cisplatin by inhibiting activation of the PI3K/AKT/NF-κB pathway, thereby promoting apoptosis and inhibiting cell migration. A comprehensive comparison of the pharmacological activities of the three components revealed that total saponins exhibited the strongest effects in all four aspects: proliferation inhibition, migration inhibition, apoptosis induction, and pathway inhibition. The IC_{50} value for the total saponins combined with cisplatin (10.21 ± 0.20 μM) was closest to that of sensitive A549 cells (9.92 ± 0.42 μM), with a reversal factor of 2.24; the apoptosis rate increased to 50.26 ± 1.33%, and the q-value for the synergistic effect was 1.38; the inhibitory

effects on PI3K, the p-AKT/AKT ratio, and NF-κB were also the most significant ($P < 0.0001$). Therefore, total saponins are the optimal sensitizing active ingredients in Jiegeng Decoction for reversing cisplatin resistance. Based on the theory of "systemic target identification and treatment," this study systematically elucidated the active components and molecular mechanisms by which Jiegeng Decoction reverses cisplatin resistance in lung cancer, identified total saponins as the optimal sensitizing active component, and confirmed that the PI3K/AKT/NF-κB pathway was the core target pathway. This discovery provides a scientific basis for the precise clinical application of Jiegeng Decoction and lays the foundation for the development of new chemotherapeutic sensitizers with total saponins from Jiegeng Decoction as the core component.

Author Contributions: Lei Shen and Guang Chen contributed to content determination, design, and writing of the article. Mengqin Zhu, Jinyu Li, Yanfeng Yuan, and Chang Yi participated in the experimental implementation and data processing. Xili Zhang and Wenlong Liu conceived the study, provided funding support, and made modifications.

Funding: This work was supported by grants from the National Natural Science Foundation of China (81874344), Hunan Province Major Scientific Research Project for High-level Talents in Health and Wellness (R2023139), Key Scientific Research Project of Hunan Provincial Department of Education (25A0275), Hengyang Science and Technology Innovation Key RD Project (202550028002), and Open Fund of the State Key Laboratory of Traditional Chinese Medicine Powders and Innovative Drugs Incubation Base (25PTKF1004).

Institutional Review Board Statement: Not applicable.

Informed Consent Statement: ANot applicable.

Data Availability Statement: The data presented in this study are available in the Supplementary Material of this article.

Acknowledgments: The authors would like to thank all members of the research team for their valuable discussions and technical support throughout this study. We are also grateful to the collaborators at Hunan University of Chinese Medicine and Hengyang Traditional Chinese Medicine Hospital for their assistance with data collection and clinical insights. Special thanks go to the funding agencies listed in the funding section for their financial support, which made this research possible.

Conflicts of Interest: The authors declare that the research was conducted in the absence of any commercial or financial relationships that could be construed as potential conflicts of interest.

Abbreviations

The following abbreviations are used in this manuscript:

AKT	Protein kinase B
AKT1	AKT serine/threonine kinase 1
BCA	Bicinchoninic acid
BP	Biological process
CC	Cellular component
CCK-8	Cell Counting Kit-8
DDP	Cisplatin
DC	Degree centrality
DL	Drug-likeness
DMEM	Dulbecco's Modified Eagle Medium
DMSO	Dimethyl sulfoxide
ECL	Enhanced chemiluminescence
ELSD	Evaporative light scattering detector
F-12K	Ham's F-12K medium

FBS	Fetal bovine serum
FPG	Total flavonoids of Jiegeng Decoction
GO	Gene Ontology
HPLC	High-performance liquid chromatography
IC_{50}	Half-maximal inhibitory concentration
KEGG	Kyoto Encyclopedia of Genes and Genomes
MF	Molecular function
NF-κB	Nuclear factor kappa-B
NFKB1	Nuclear factor kappa B subunit 1
NSCLC	Non-small cell lung cancer
OB	Oral bioavailability
PBS	Phosphate-buffered saline
PDA	Photodiode array detector
PI3K	Phosphoinositide 3-kinase
PIK3CA	Phosphatidylinositol-4,5-bisphosphate 3-kinase catalytic subunit alpha
PPI	Protein-protein interaction
PPG	Total polysaccharides of Jiegeng Decoction
PVDF	Polyvinylidene fluoride
SDS-PAGE	Sodium dodecyl sulfate-polyacrylamide gel electrophoresis
SPG	Total saponins of Jiegeng Decoction
TBST	Tris-buffered saline with Tween 20
TCMSP	Traditional Chinese Medicine Systems Pharmacology Database
UV	Ultraviolet spectrophotometry

References

1. Meng F, Raoof M. Global cancer statistics 2022: GLOBOCAN estimates of incidence and mortality worldwide for 36 cancers in 185 countries-Reply. Gastroenterology. 2026;170(2):432-3. http://dx.doi.org/10.1053/j.gastro.2025.10.014.

2. Rocca A, Crinò L, Braga L, Salton F, Ruaro B, Confalonieri M, et al. Refining treatment strategies for non-small cell lung cancer lacking actionable mutations: insights from multi-omics studies. British Journal of Cancer. 2025;133(10):1405-27. http://dx.doi.org/10.1038/s41416-025-03139-6.

3. Yang KH, Hua SS, Wei WT, Yang CY, Zhu XH, Li SC. Economic burden of advanced lung cancer patients treated by gefitinib alone and combined with chemotherapy in two regions of China. Journal of Medical Economics. 2023;26(1):1424-31. http://dx.doi.org/10.1080/13696998.2023.2272536.

4. Sun L, Marmarelis ME, Langer CJ. Systemic Therapy for Mutation-Driven NSCLC. Seminars in Radiation Oncology. 2021;31(2):140-8. http://dx.doi.org/10.1016/j.semradonc.2020.11.011.

5. Ettinger DS, Wood DE, Aisner DL, Akerley W, Bauman JR, Bharat A, et al. Non-Small Cell Lung Cancer, Version 2.2021 Featured Updates to the NCCN Guidelines. Journal of the National Comprehensive Cancer Network. 2021;19(3):254-66. http://dx.doi.org/10.6004/jnccn.2021.0013.

6. Zhou HR, Zhang MX, Cao HH, Du XT, Zhang X, Wang J, et al. Research Progress on the Synergistic Anti-Tumor Effect of Natural Anti-Tumor Components of Chinese Herbal Medicine Combined with Chemotherapy Drugs. Pharmaceuticals. 2023;16(12). http://dx.doi.org/10.3390/ph16121734.

7. Zhang L, Wang Y, Yang D, Zhang C, Zhang N, Li M, et al. Platycodon grandiflorus - an ethnopharmacological, phytochemical and pharmacological review. J Ethnopharmacol. 2015;164:147-61. http://dx.doi.org/10.1016/j.jep.2015.01.052.

8. Fu Y, Xin Z, Liu B, Wang J, Wang J, Zhang X, et al. Platycodin D Inhibits Inflammatory Response in LPS-Stimulated Primary Rat Microglia Cells through Activating LXRα-ABCA1 Signaling Pathway. Front Immunol. 2017;8:1929. http://dx.doi.org/10.3389/fimmu.2017.01929.

9. So-Hee H, Jae-Han L, Joong-Seok W, Gi-Hwan J, Soo-Hyun J, Eun-Ji H, et al. Platycodin D induces apoptosis via regulating MAPK pathway and promotes autophagy in colon cancer cell. Biomedicine & Pharmacotherapy. 2024;172:116216. http://dx.doi.org/https://doi.org/10.1016/j.biopha.2024.116216.

10. Ni Z, Dawa Z, Suolang D, Pingcuo Q, Langga Z, Quzhen P, et al. Platycodin D inhibits the proliferation, invasion and migration of endometrial cancer cells by blocking the PI3K/Akt signaling pathway via ADRA2A upregulation. Oncol Lett. 2023;25(4):136. http://dx.doi.org/10.3892/ol.2023.13722.

11. Peng Y, Cheng PF, Fan JY, Zheng AH, Deng DP, Li QH. Platycodin D Overcomes Cisplatin Resistance in Gastric Cancer by Inducing Ferroptosis through TLK1-Dependent UHRF2/DNMT3A/ALOX15 Pathway. Chinese Journal of Integrative Medicine. 2026. http://dx.doi.org/10.1007/s11655-026-3848-y.

12. Qiuyan G, Minghong Z, Qixin W, Tianming L, Piao L, Lin C, et al. Glycyrrhetinic acid inhibits non-small cell lung cancer via promotion of Prdx6- and caspase-3-mediated mitochondrial apoptosis. Biomedicine & Pharmacotherapy. 2024;173:116304. http://dx.doi.org/https://doi.org/10.1016/j.biopha.2024.116304.

13. Shengjie H, Wenjing F, Jierong P, Ruijiao D, Chengjuan L, Miaomiao J. The effect of Jiegeng decoction on lipopolysaccharide-induced acute lung injury in mice based on metabolomics. Acta Pharmaceutica Sinica. 2023;58(7):1913-21. http://dx.doi.org/10.16438/j.0513-4870.2022-1295.

14. Pengfei H, Shengchen D, Hua B, Xianzhang H, Chaoyun Z. Effect of totalsaponins of Radix Platycodonis Decoction on IKK/NF-KB/MUC5AC pathway in rats with chronic obstructive pulmonary disease. Chinese Journal of Hospital Pharmacy. 2021;41(12):1197-201+207. http://dx.doi.org/10.13286/j.1001-5213.2021.12.03.

15. Chen W, Liu XQ, Yuan SJ, Qiao TK. HSPA12B overexpression induces cisplatin resistance in non-small-cell lung cancer by regulating the PI3K/Akt/NF-κB signaling pathway. Oncology Letters. 2018;15(3):3883-9. http://dx.doi.org/10.3892/ol.2018.7800.

16. Yu ML, Qi BQ, Wu XX, Xu J, Liu XL. Baicalein increases cisplatin sensitivity of A549 lung adenocarcinoma cells via PI3K/Akt/NF-κB pathway. Biomedicine & Pharmacotherapy. 2017;90:677-85. http://dx.doi.org/10.1016/j.biopha.2017.04.001.

17. Chen BS, Shen ZJ, Wu DG, Xie X, Xu X, Lv LZ, et al. Glutathione Peroxidase 1 Promotes NSCLC Resistance to Cisplatin via ROS-Induced Activation of PI3K/AKT Pathway. Biomed Research International. 2019;2019. http://dx.doi.org/10.1155/2019/7640547.

18. Li YG, Song X, Niu JT, Ren MM, Tang GJ, Sun Z, et al. Pentraxin 3 acts as a functional effector of Akt/NF-κB signaling to modulate the progression and cisplatin-resistance in non-small cell lung cancer. Archives of Biochemistry and Biophysics. 2021;701. http://dx.doi.org/10.1016/j.abb.2021.108818.

19. Feng Y, Jiang Y, Yang L, Lu D, Li N, Zhang Q, et al. Interactions and communications in lung tumour microenvironment: chemo/radiotherapy resistance mechanisms and therapeutic targets. J Drug Target. 2025;33(6):817-36. http://dx.doi.org/10.1080/1061186x.2025.2453730.

20. Liu R, Chen YW, Liu GZ, Li CX, Song YR, Cao ZW, et al. PI3K/AKT pathway as a key link modulates the multidrug resistance of cancers. Cell Death & Disease. 2020;11(9). http://dx.doi.org/10.1038/s41419-020-02998-6.

21. Abolfathi H, Arabi M, Sheikhpour M. A literature review of microRNA and gene signaling pathways involved in the apoptosis pathway of lung cancer. Respiratory Research. 2023;24(1). http://dx.doi.org/10.1186/s12931-023-02366-w.

22. Jinjun S, Rui Y, Xinzhuang Z, Cunsi S, Jianjian J, Tong X, et al. Network pharmacological study of antitussive and expectorant effective of Jiegeng Decotion. Chinese Traditional and Herbal Drugs. 2018;49(15):3501-8.

23. Vermeer PD, Denker J, Estin M, Moninger TO, Keshavjee S, Karp P, et al. MMP9 modulates tight junction integrity and cell viability in human airway epithelia. Am J Physiol Lung Cell Mol Physiol. 2009;296(5):L751-62. http://dx.doi.org/10.1152/ajplung.90578.2008.

24. Xinyu Z, Yuanhan Z, Yan F, Xuemei Z, Shouwen Z, Jinxiang Z. Study on the antitussive and expectorant activities and mechanism of platycodin D based on metabolomics method. Acta Pharmaceutica Sinica. 2024;59(3):724-34. http://dx.doi.org/10.16438/j.0513-4870.2023-0744.

25. Wang B, Gao Y, Zheng G, Ren X, Sun B, Zhu K, et al. Platycodin D inhibits interleukin-13-induced the expression of inflammatory cytokines and mucus in nasal epithelial cells. Biomed Pharmacother. 2016;84:1108-12. http://dx.doi.org/10.1016/j.biopha.2016.10.052.
26. Jinling Z, Xinyue L, Pin Z. Influence of glycyrrhitic acid on the expression of matrix metalloproteinase-2 and matrix metalloproteinase-9 in leukemia cell lines K562. Chinese Journal of Hospital Pharmacy. 2009;29(8):613-6.
27. Yuan L. Screening bioactive compounds of Jiegeng decoction and revealing dynamic behavior of target-components: Northwest University; 2019.
28. Charlton CL, Babady E, Ginocchio CC, Hatchette TF, Jerris RC, Li Y, et al. Practical Guidance for Clinical Microbiology Laboratories: Viruses Causing Acute Respiratory Tract Infections. Clin Microbiol Rev. 2019;32(1). http://dx.doi.org/10.1128/cmr.00042-18.
29. Yuqian Z, Ronghua W, Xiang C, Yan Y, Pinghu Z. Research Progress of TLR-4 Signaling Pathway Mediated Acute Lung Injury and ARDS Caused by Viral Infection. Chinese Journal of Virology. 2021;37(5):1234-43. http://dx.doi.org/10.13242/j.cnki.bingduxuebao.003887.
30. Commission CP. Pharmacopoeia of the People's Republic of China (2025 Edition) — Part I: Beijing: China Medical Science Press; 2025. 1945 p.
31. Bin S, Zhen L, Chiyu J. Progress in the research of the relationship between acute lung injury or acute respiratory distress syndrome and nuclear factor kappa B signaling pathway. Chinese Journal of Injury Repair and Wound Healing(Electronic Edition). 2016;11(2):147-50.
32. Zhao J, Hou M, Ding K, Li S, Li H, Zhang X, et al. Jie Geng Tang reverses cisplatin resistance through the Nrf2 pathway in lung cancer. J Pharm Pharmacol. 2023;75(6):784-805. http://dx.doi.org/10.1093/jpp/rgad018.
33. Wang D, Cheng J, Zhang J, Zhou F, He X, Shi Y, et al. The Role of Respiratory Microbiota in Lung Cancer. Int J Biol Sci. 2021;17(13):3646-58. http://dx.doi.org/10.7150/ijbs.51376.
34. Shunlai Q, Yonggang Z, Delong D. Effects of Glycyrrhizin on Proliferation, Migration, and Invasion of Nasopharyngeal Carcinoma 6-10B Cells via Regulating circ0009910 Expression. Chinese Journal of Gerontology. 2023;43(17):4276-9.
35. Yuan H, Yanyun G, Xinrui C. Advances in the pathogenesis of idiopathic pulmonary fibrosis. Chinese Journal of Medicine. 2024;59(10):1054-9.
36. Li Y, Wang ZH, Wang S, Zhao JH, Zhang JB, Huang YJ. Gremlin-mediated decrease in bone morphogenetic protein signaling promotes aristolochic acid-induced epithelial-to-mesenchymal transition (EMT) in HK-2 cells. Toxicology. 2012;297(1-3):68-75. http://dx.doi.org/10.1016/j.tox.2012.04.004.
37. Di L. Antagonisms and Mechanisms of Bone Morphogenetic Protein-7 on Silica-induced Pulmonary Fibrosis through Modulating the Balance of Smad Signaling Pathway: Capital Medical University; 2016.
38. Lufang N. Syndrome Differentiation Rules of Zhang Zhongjing in Treating Pulmonary Atrophy and Related Experimental Studies: Beijing University of Chinese Medicine; 2007.
39. Li B, Jiang X, Liu C, Ma Y, Zhao R, Zhang H. Exploring the preventive effects of Jie Geng Tang on pulmonary fibrosis induced in vitro and in vivo: a network pharmacology approach. Naunyn-Schmiedeberg's Archives of Pharmacology. 2024;397:10005 - 16.
40. Kanehisa M, Furumichi M, Sato Y, Matsuura Y, Ishiguro-Watanabe M. KEGG: biological systems database as a model of the real world. Nucleic Acids Research. 2024;53(D1):D672-D7. http://dx.doi.org/10.1093/nar/gkae909.
41. Kanehisa M. Toward understanding the origin and evolution of cellular organisms. Protein Science. 2019;28(11):1947-51. http://dx.doi.org/10.1002/pro.3715.
42. Kanehisa M, Goto S. KEGG: kyoto encyclopedia of genes and genomes. Nucleic Acids Res. 2000;28(1):27-30. http://dx.doi.org/10.1093/nar/28.1.27.

43. Ruolin Z, Kunfu Z, Xu Z, Meijuan C. Research on mechanisms of PD-induced inhibition of adhesion,invasion and migration in non-small cell lung cancer H460 and A549 cells. Chinese Pharmacological Bulletin. 2015;31(2):241-7.
44. Shen JF, Dai ZY, Li YS, Zhu HP, Zhao LJ. TLR9 regulates NLRP3 inflammasome activation via the NF-kB signaling pathway in diabetic nephropathy. Diabetology & Metabolic Syndrome. 2022;14(1). http://dx.doi.org/10.1186/s13098-021-00780-y.
45. Chaoyun Z, Pengfei H, Shengchen D, Zhongming Z. Effect of Total Flavonoids of Jiegeng Decoction on TLR4/TRIF/IRF3 Pathway in Rats with Chronic Obstructive Pulmonary Disease. Modernization of Traditional Chinese Medicine and Materia Medica-World Science and Technology. 2022;24(4):1495-502.
46. Hongyan W. Study on the Mechanism of Platycodon grandiflorus Decoction in the Treatment of Acute Lung Injury Based on UPLC-Q-TOF-MS/MS and Network Pharmacology: Anhui University of Chinese Medicine; 2023.
47. Xiaoyan Z, Guangwei Z. Correlation Study on the Compatibility and Pharmacological Effects of the Jieg-eng-Gancao Herb Pair. China's Naturopathy. 2014;22(8):58-9. http://dx.doi.org/10.19621/j.cnki.11-3555/r.2014.08.054.
48. Guanglei W. Research and Exploration on Jiegeng Decoction in the Treatment of Cough. Medical Diet and Health. 2020;18(23):178-9.

Supplementary Files

This is a list of supplementary files associated with this preprint. Click to download.

- GraphicalAbstract.jpg